Topoisomerase III-alpha in Double Holliday Junction Dissolution

by

Stefanie Lynn Hartman Chen

Department of Biochemistry
Duke University

Date:_____

Approved:

_____
Tao-shih Hsieh, Supervisor

_____
Arno L. Greenleaf

_____
Kenneth N. Kreuzer

_____
David MacAlpine

_____
Jane S. Richardson

_____
Laura Rusche

Dissertation submitted in partial fulfillment of
the requirements for the degree of Doctor of Philosophy in the Department of
Biochemistry in the Graduate School
of Duke University

2012

ABSTRACT

Topoisomerase III-alpha in Double Holliday Junction Dissolution

by

Stefanie Lynn Hartman Chen

Department of Biochemistry
Duke University

Date:_____

Approved:

_____
Tao-shih Hsieh, Supervisor

_____
Arno L. Greenleaf

_____
Kenneth N. Kreuzer

_____
David MacAlpine

_____
Jane S. Richardson

_____
Laura Rusche

An abstract of a dissertation submitted in partial
fulfillment of the requirements for the degree
of Doctor of Philosophy in the Department of
Biochemistry in the Graduate School
of Duke University

2012

Abstract

Topoisomerase IIIα (Top3α) is an essential component of the double Holliday junction (dHJ) dissolvasome complex in metazoans. Previous work has shown that Top3α and Bloom's helicase (Blm) are able to convergently migrate the dHJ to create solely non-crossover products, thus preserving genomic integrity. However, many questions remain about the details of this process. Using a combination of biochemical and genetic tools, including dHJ substrate assays, gel electrophoresis, EMSA, pulldowns, fly crosses, and electron microscopy, this work expands our knowledge of the dissolution reaction. Tail mutants of Top3α were created and tested in a series of *in vitro* assays. Through these experiments, I discovered that the C-terminus of Top3α is important for binding Blm, interacting with DNA, conveying RPA stimulation, and *in vivo* functionality. I also observed that dissolution is an extremely processive reaction, with no accumulation of intermediates prior to product formation. When a non-specific topoisomerase was used (Top1, a type IB), accumulation of an intermediate was evident; however, contrary to predicted models, direct observation revealed that this intermediate is not a hemicatenane structure and still requires branch migration. Modifications were also made to the dHJ substrate creation method so that multiple types of HJ substrates could be produced efficiently.

Dedication

To Dr. Jody L. Plank, without whom this never would have happened.

Contents

List of Tables

List of Figures

Acknowledgements

I would like to first and foremost thank my mentor, Dr. Tao-shih Hsieh, who has provided immense support both personally and professionally throughout this endeavor.

I would also like to thank my lab mates throughout my time in the Hsieh lab, who were both great companions and great scientific minds. In addition, I would like to thank the Kuehn lab for taking me in as a surrogate lab when the Hsieh lab was dwindling.

For keeping me sane, I am indebted to both Duke Chinese Dance Troupe and the Hidden Mountain Bujinkan Dojo. Both provided great opportunities for stress relief, leadership, and lifelong friends.

I also need to thank my family for their support. My parents introduced me early on to DNA (largely through their creative Life Technologies t-shirts) and encouraged me to work hard and think logically, which are invaluable skills. My brother was always there to make sure I didn't take myself too seriously.

The support of my husband, Vincent Chen, means more to me than I can say. He has provided a sympathetic ear, a shoulder to cry on, comic relief, and most of my meals throughout graduate school. *Wo ai ni.*

1. Introduction

1.1 Topoisomerase IIIα

1.1.1 Top3α is a type IA topoisomerase

Top3α is a member of the type IA topoisomerase family, which is defined by several structural and mechanistic features. Type IA topoisomerases bind to single-stranded DNA and transiently cleave the single strand to allow another to pass through, before reversing the reaction and re-ligating the backbone strand. The active site tyrosine covalently attaches to the phosphate on the 5' side of the strand, while the 3' end is nestled into a positively-charged groove on the opposite side of the protein gate. A hinging motion of the protein allows the cleaved backbone to separate enough for another strand of DNA to pass through (Figure 1C). Due to the strand passage mechanism, type IA topoisomerases change the linking number (*Lk*) in distinct steps of 1 (Table 1). (CHAMPOUX, 2001)

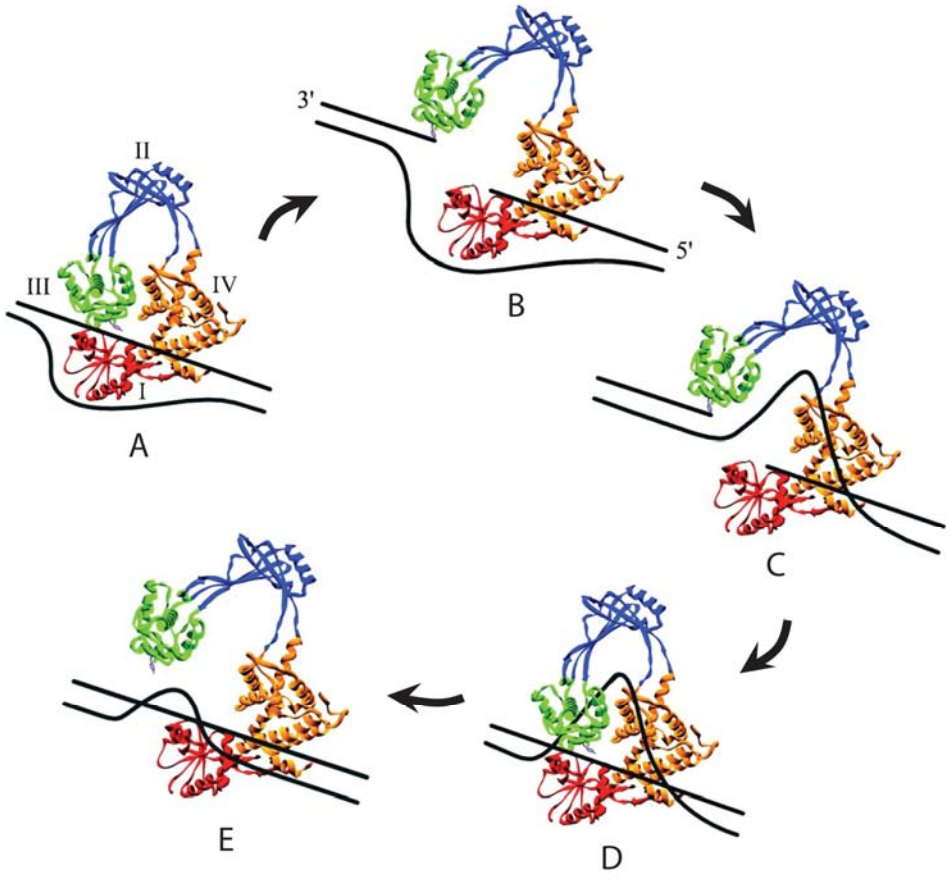

Figure 1: Mechanism of type IA topoisomerases.
The topoisomerase is shown as a ribbon diagram, and each black line is one strand of DNA. The four conserved domains are labeled in (A). Adapted from *Annual Reviews in Biochemistry* (CHAMPOUX, 2001).

The active site regions of type IA topoisomerases share a set of domains, known as I-IV, that form a distinct toroidal structure (Figure 1A). The active site tyrosine is located in domain III, while the ssDNA binding groove is located between domains I & IV. Domain II forms the top of the toroid. The enzyme "hinge" is located between domains II & IV. The additional C-terminal domain (in enzymes that have one) extends out from domain I.

The type IA mechanism is passive, meaning that the DNA itself provides the energy and directionality for strand passage. Using a hyper-negatively supercoiled substrate (which contains single-stranded regions due to the extreme underwinding of the helix), relaxation will cease after the substrate has transitioned to negatively supercoiled (the level maintained in cells), due to the absence of single-stranded regions. However, given a substrate with a permanently denatured region (*i.e.* a bubble), the topoisomerase can catalyze complete relaxation of either positively or negatively supercoiled, covalently closed substrates (PLANK ET AL., 2005).

Type IA topoisomerases can also perform decatenation of single strands, with *Ec*Top3 showing a stronger activity than *Ec*Top1 (HIASA ET AL., 1994). In conjunction with RecQ helicase, *Ec*Top3 can also fully catenate plasmid DNA by passing one melted strand at a time (HARMON ET AL., 1999). Top3α can also decatenate single-stranded circles, and this activity is enhanced by Blm (a RecQ homologue) and Rmi1 (YANG ET AL., 2010).

Whether the type IA topoisomerases can accommodate a double strand in the toroid during strand passage (as in a D-loop structure), or if it strictly requires a single strand, remains unclear. Because the size of the toroid is approximately 25 Å across, and the diameter of a DNA helix is 20 Å, accommodation of a duplex remains theoretically possible.

The type IA family includes the first topoisomerase to be discovered, originally called ω protein and now known as prokaryotic Top1. Bacteria have two type IA members: Top1 and Top3. In eukaryotes, Top1 is a type IB topoisomerase, which is mechanistically very different from type IA (Table 1). Yeast have just one type IA: Top3. Metazoans have both Top3α and Top3β, which are similar type IA enzymes encoded in separate genes. In both prokaryotes and metazoans, the two type IA enzymes share their conserved N-termini, which contain the active site region, including domains I-IV, and differ in their C-terminal regions (Figure 3).

Table 1: Categories of topoisomerases.

Type	Mechanism	Example
IA	Binds ssDNA and performs strand passage, $\Delta Lk = 1$	Prokaryotic Top1, Top3's
IB	Binds dsDNA and allows rotation, $\Delta Lk > 1$	Eukaryotic Top1
IC	Binds dsDNA and allows rotation, $\Delta Lk > 1$	Archaeal Top5
IIA	Forms a homodimer, binds dsDNA and passes one helix through another, $\Delta Lk = 2$	Eukaryotic Top2, prokaryotic Top4
IIB	Forms a heterodimer, binds dsDNA and passes one helix through another, $\Delta Lk = 2$	Archaeal Top6

1.1.2 Phenotypes of Top3α

Top3α is an essential gene in mice, highlighting its biological importance. Top3α knockout mice die *in utero*, and even cultured embryos show a severe growth limitation

(LI & WANG, 1998). Top3α is also essential in *Drosophila*, with flies homozygous for a hypomorphic mutant dying during the pupae stage (PLANK ET AL., 2005).

To determine the cause of cell death, an inducible-off system was designed in DT40 cells. When Top3α was turned off, the cells stopped dividing after three days and then slowly died off. A large number of cells arrested in G2 phase, presumably from a DNA damage checkpoint, and highly aberrant chromosomes were observed, indicating an essential role in preserving genome stability (SEKI ET AL., 2006).

In addition to its nuclear role, Top3α is also expressed as a longer isoform that localizes to the mitochondria (WANG ET AL., 2002), where it likely functions in mtDNA replication. Due to the temporal delay between firing of the origins on the two strands of the mtDNA genome, a single-stranded region remains for a large part of the replication process (BROWN, 2005), allowing separation of the daughter genomes by a type IA topoisomerase. *Drosophila* containing Top3α that lacks the mitochondrial localization sequence have a lower mtDNA copy number and ATP content as well as fertility defects (WU ET AL., 2010). Specifically, females are sterile, and male fertility is greatly reduced due to fewer viable germline stem cells. Therefore, Top3α appears to be critical to the effective energy production of mitochondria, especially in cells which require high energy loads.

In contrast to Top3α, its isozyme Top3β is far from essential. Mice knockouts of Top3β develop to adulthood without any major issues (KWAN & WANG, 2001). Over

several generations, their fecundity decreases and some develop autoimmunity (KWAN ET AL., 2003; KWAN ET AL., 2007). This drastic difference in biological function, despite having identical type IA activities *in vitro* (WILSON ET AL., 2000; PLANK ET AL., 2005), indicates that Top3α has a unique role in the cell.

Yeast have only one type IA, Top3, which is not essential. However, Top3 mutants are slow growing and demonstrate hyperrecombination (WALLIS ET AL., 1989). In addition, the deletion strain exhibited an increase in chromosome nondisjunction, smaller cell sizes, and decreased formation of diploids and spores. These phenotypes are suppressed by deleting Sgs1, the sole RecQ-family helicase present in yeast (GANGLOFF ET AL., 1994), indicating that the two enzymes act in the same pathway.

1.1.3 Top3α interacts with Bloom's helicase

Similar to the yeast, human Top3α co-immunoprecipitates Blm, a RecQ helicase in humans, and the two proteins co-localize to nuclear foci (JOHNSON ET AL., 2000). Blm is able to stimulate the *in vitro* relaxation activity of Top3α approximately two-fold, although this was dependent on the presence of RPA (replication protein A, the eukaryotic single-stranded DNA binding protein) (WU & HICKSON, 2002). The actions and implications of this protein complex will be discussed in more detail, following an overview of the activities and functions of Blm.

1.2 Bloom's helicase

1.2.1 Blm is a RecQ family helicase

Blm is a member of the RecQ family of Superfamily 2 helicases. It contains a DEAH-box helicase domain with seven conserved motifs, a RecQ family C-terminal domain (RQC), and a helicase RNase D C-terminal domain (HRDC) (COBB & BJERGBAEK, 2006). Yeast contain one member (Sgs1) while humans have five (RecQ1, Blm, WRN, RecQ4, and RecQ5), three of which are associated with disease (Blm, WRN, and RecQ4). *Drosophila* species contain three: Blm, RecQ4, and RecQ5. The founding member, *E. coli* RecQ, is involved in the RecF recombination pathway and suppresses illegitimate recombination (HANADA ET AL., 1997).

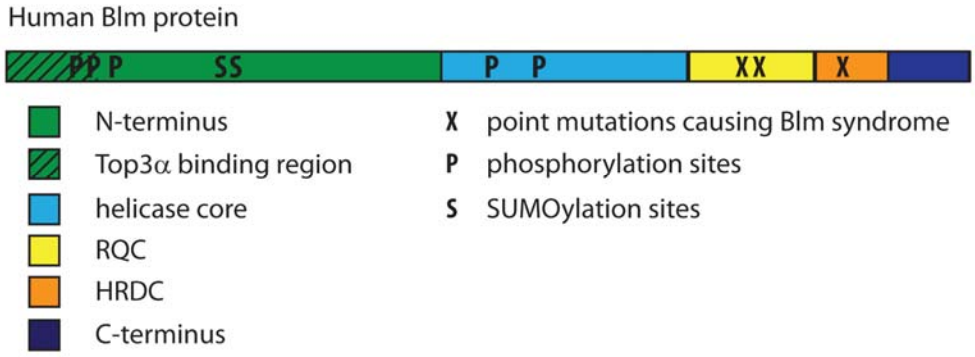

Figure 2: Domains and post-translational modifications of Blm helicase.

Like all RecQ family members, Blm is a 3'-5' helicase (KAROW ET AL., 1997). However, it is not very processive, unwinding only duplex substrates under 100 bp; the addition of RPA specifically stimulates the helicase activity, allowing unwinding of a few hundred base pairs (BROSH ET AL., 2000). Blm, like other RecQ helicases, prefers

more complex DNA substrates, efficiently unwinding both G-quadruplex (SUN ET AL., 1998) and D-loop structures (BACHRATI ET AL., 2006). Blm also possesses strand annealing activity in its N-terminus (CHEN & BRILL, 2010), and the combination of helicase and strand annealing activities likely contribute to its Holliday junction branch migration activity. Blm prefers binding to Holliday junctions over duplex or tailed DNA and can migrate a junction over 2 kb (KAROW ET AL., 2000).

The RQC and HRDC domains appear to be involved in binding specialized DNA substrates, as each individually binds tightly to G-quadruplex DNA as well as Holliday junctions and forks (HUBER ET AL., 2006).

In addition to strand annealing, the N-terminus of Blm has been implicated in a variety of protein-protein interactions, including Rad51, RPA, Top3α, Rmi1 & Rmi2. This region has also been implicated in interaction between Blm monomers, forming a hexamer when isolated (BERESTEN ET AL., 1999). Electron microscopy of full-length Blm has also revealed tetramer and hexamer arrangements (KAROW ET AL., 1999). However, a recent study showed that the monomer form provides the maximal helicase activity, while maximal branch migration occurred with three to four monomers (MAZINA ET AL., 2012). The exact multimeric conformation *in vivo* is unknown, and may vary according to the function that Blm is performing.

Blm is phosphorylated at two threonines in the N-terminus (T99 & T122) by both ATM and ATR in response to DNA damage (BEAMISH ET AL., 2002; DAVIES ET AL., 2004),

but the exact role of the modification is unclear. Cells containing non-phosphorylable Blm mutants arrest in G2 following exposure to hydroxyurea, indicating a defect in recovering from replication failure; however, the mutant was still able to suppress sister chromatid exchanges (SCE's, a hallmark of Blm deficiency, see below) and colocalize with Top3α, Rad51, PCNA, and γH2AX (DAVIES ET AL., 2004). In addition to damage-specific phosphorylation, Blm is also phosphorylated in a cell cycle dependent manner. The mitotic kinases MPS1 and Cdc2 kinase phosphorylate residues S144 and S714 & T766, respectively (BAYART ET AL., 2006; LENG ET AL., 2006). Similar to above, non-phosphorylable mutants did not have increased SCE's, but displayed problems with chromosome segregation. Blm is also SUMOylated at two sites in the N-terminus (Figure 2) (OUYANG ET AL., 2009). The SUMOylation appears to be required for recruitment of Rad51 to sites of replication failure.

Levels of Blm increase during S phase, are maintained in G2/M phase, and are very low during G1 phase, consistent with roles in replication and recombination (DUTERTRE ET AL., 2000).

1.2.2 Phenotypes of Blm

The Blm helicase is named after Bloom's syndrome, which is a recessive autosomal disorder characterized by an increase in all types of cancers, proportional dwarfism, immunodeficiency, and partial sterility (GERMAN, 1993).

On the cellular level, Bloom's syndrome is characterized by a greater than 10-fold increase in sister chromatid exchanges (SCE's), which are visualized as harlequin chromosomes (CHAGANTI ET AL., 1974). A dramatic increase in somatic recombination was also shown by the 50- to 100-fold increase of mutations in glycophorin A on erythrocytes of human Bloom syndrome patients (LANGLOIS ET AL., 1989).

Similar phenotypes are seen in a Bloom syndrome mouse model. Although some Blm mutant mice died during gestation, others lived to adulthood, replicating the human syndrome (CHESTER ET AL., 1998; LUO ET AL., 2000). Adult Bloom syndrome mice showed a ten-fold increase in SCE's, predisposition towards cancers (29% had a tumor by 20 months of age), and an 18-fold increase in loss of heterozygosity (LOH), which is an expected effect of increased somatic recombination (LUO ET AL., 2000).

Drosophila knockouts of the mus309 gene (encoding the Blm homologue protein) similarly show increased mutagen sensitivity, increased chromosome loss and nondisjunction, and defects in fertility (KUSANO ET AL., 2001). Blm mutant flies also exhibit a greater than 50-fold increase in crossover events, which can be mitigated by additionally mutating Rad51, indicating a role in the homologous recombination pathway (JOHNSON-SCHLITZ & ENGELS, 2006). Blm mutants were also synthetic lethal with the crossover junction endonuclease Mus81, indicating a role in Holliday junction resolution.

1.2.3 Blm is involved in many pathways

On the molecular level, Blm is involved with numerous partner proteins in a variety of genome stability pathways (Table 2).

Table 2: Blm interacting proteins.

Blm-Interacting Protein	Protein Function	Function with Blm	Reference
ATM	DNA damage kinase (double-strand breaks)	Phosphorylates Blm in response to DNA damage	(BEAMISH ET AL., 2002)
ATR	DNA damage kinase (replication failure)	Phosphorylates Blm in response to DNA damage	(DAVIES ET AL., 2004)
Exo1	5'-3' exonuclease	Blm stimulates processivity	(NIMONKAR ET AL., 2008)
FANCJ	5'-3' helicase	Recycle histones during synthesis/transcription	(SARKIES & SALE, 2011; SUHASINI & BROSH, 2012)
Fen1	Flap endonuclease	Blm stimulates nuclease	(SHARMA ET AL., 2004)
Mlh1	Part of MutLγ	Promote meiotic crossovers	(ZAKHARYEVICH ET AL., 2012)
Mus81	HJ endonuclease	Blm stimulates nuclease activity	(ZHANG ET AL., 2005)
p53	Tumor suppressor	Inhibits dHJ binding and helicase activity of Blm	(YANG ET AL., 2002)
PICH	Nucleosomoe remodeling	Prevent histone association with uncatenated DNA	(KE ET AL., 2011)
Rad51	Promotes strand invasion to initiate HR	Blm reduces Rad51 foci	(WU ET AL., 2001)
Rad54	Chromatin remodeller	Blm promotes Rad54 activity, blocks Rad54-Rad51 interaction	(SRIVASTAVA ET AL., 2009)
RNA Pol I	rRNA transcription	Blm melts GC-rich rDNA regions	(GRIERSON ET AL., 2011)
RPA	ssDNA binding protein	Enhances Blm processivity	(BROSH ET AL., 2000)
Top2α	DNA relaxation	Enhances Blm helicase activity on overhangs and bubbles	(RUSSELL ET AL., 2011)
Top3α	ssDNA strand passage	dHJ dissolution	(WU & HICKSON, 2003; PLANK ET AL., 2006)
Complex	**Components**	**Function**	**Reference**
BASC	BRCA1, Msh2, Msh6, Mlh1, ATM, Blm, Rad50-Mre11-Nbs1, RFC	Sense and repair damage during DNA replication	(WANG ET AL., 2000)
BRAFT	Blm, RPA, FANCA, FANCC, FANCE, FANCF, FANCG, Top3α	Genome stability	(MEETEI ET AL., 2003)

Blm has a role in the restart of stalled replication forks. It has been demonstrated that Blm is able to regress a model replication fork into a chickenfoot structure (RALF ET AL., 2006), which would allow for template switching or recombination-mediated re-initiation of replication. Cells lacking Blm are defective in replication fork recovery and are more likely to fire new origins while under replicative stress (DAVIES ET AL., 2007), indicating an additional role in suppression of new origin firing.

Blm is required for efficient rRNA transcription; it interacts with RNA Pol I at the promyelocytic leukemia (PML) protein bodies and unwinds GC-rich regions ahead of the polymerase (GRIERSON ET AL., 2011). Blm is also important for protecting the gene cluster stability of the rDNA repeats, as Blm mutants show a 100-fold increase in spontaneous alterations to the gene cluster architecture, due to their inability to prevent non-allelic homologous recombination (KILLEN ET AL., 2009).

Blm has several roles in the initiation of recombinational repair. Independent of its helicase activity, Blm specifically stimulates the resection activity of Exo1 (which is not very processive alone) to create a 3' protruding end (NIMONKAR ET AL., 2008). The 3' tail is the substrate for strand invasion by Rad51, and a longer exposed tail increases the fidelity of the homology search. Blm can dissociate Rad51-nucleoprotein complexes when Rad51 is in the inactive, ADP-bound state (BUGREEV ET AL., 2007); in contrast, Blm assists Rad51 with strand exchange when Rad51 is in its active (ATP-bound) form (BUGREEV ET AL., 2009). Blm is also able to efficiently unwind D-loops (BACHRATI ET AL.,

2006), which are the product of Rad51 strand invasion. In this way, Blm is able to both promote homologous recombination and prevent illegitimate recombination.

In several species, Blm (or its homologue) suppresses homeologous recombination. In yeast, Sgs1 and the mismatch repair machinery (Msh2 & Msh6) are involved in heteroduplex rejection (MYUNG ET AL., 2001; SUGAWARA ET AL., 2004). In *Drosophila*, recombination between sequences with only 81% identity was increased five-fold in the absence of Blm, and the mismatch repair machinery was not involved (KAPPELER ET AL., 2008). However, in humans, only Msh2 appears to function in this role (LAROCQUE & JASIN, 2010), highlighting a species-specific difference in Blm functions.

Several lines of evidence show that Blm is needed to resolve Holliday junctions (HJ's). Yeast lacking Sgs1 accumulate X-structures that can be resolved by expressing HJ resolvases from other species (MANKOURI ET AL., 2011). In *Drosophila*, Blm is synthetic lethal with any of the three HJ resolvases (Mus81-Eme1, Slx1-Slx4, Gen1) (ANDERSEN ET AL., 2011), while in humans, a similar effect is seen when any two of the HJ resolvases, in addition to Blm, are knocked down (WECHSLER ET AL., 2011). In contrast to its mitotic function, Sgs1 appears to be involved in creating crossovers during meiosis, in conjunction with Exo1 and MutLγ (ZAKHARYEVICH ET AL., 2012).

As mentioned above, Blm also interacts with Top3α. These enzymes act in a unique double Holliday junction dissolution process, which will be discussed in the next section. Blm lacking the N-terminal Top3α-interacting domain was no longer able to

suppress the formation of SCE's (HU ET AL., 2001), although the role of other proteins binding in this area cannot be ruled out. In yeast, a more severe phenotype was observed with active Sgs1 missing the interaction domain than with helicase-inactive Sgs1 that maintained the ability to bind Top3 (WEINSTEIN & ROTHSTEIN, 2008). These observations indicate a vital role for this protein complex.

1.3 The "BTR" Complex

1.3.1 Top3α and Blm function on double Holliday junctions

Because the effects of Blm mutants were mitigated by additionally deleting the homologous recombination initiator Rad51, and Blm was synthetic lethal with the structure-specific endonuclease Mus81 (JOHNSON-SCHLITZ & ENGELS, 2006), it was suggested that Blm acts on Holliday junctions. Blm had also been shown to bind and migrate Holliday junctions *in vitro* (KAROW ET AL., 2000; MAZINA ET AL., 2012); however, since Blm has no nuclease activity, it is unable to resolve the junctions on its own. Since Top3 was seen to act downstream of Sgs1, it seemed likely that the topoisomerase was providing the strand separating function. The ability of Blm to suppress crossovers also indicated that Blm functioned in a non-crossover resolution pathway.

Blm and Top3α were shown to resolve a double Holliday junction-like structure *in vitro* (WU & HICKSON, 2003). Further study with a topologically constrained substrate containing two migratable Holliday junctions revealed that Blm and Top3α migrate the junctions towards and through each other, separating the two molecules and resulting in

purely non-crossover products (PLANK ET AL., 2006). Because this method is distinct from classic HJ resolvases, which cleave DNA strands at the junction and create both crossovers and non-crossovers, this process was termed "dissolution."

1.3.2 Rmi proteins as part of the complex

Recent screens have found a number of non-enzymatic additions to the Blm-Top3α complex. These small associating proteins have been termed Rmi, for RecQ-mediated genome instability, and contain OB (oligonucleotide or oligosaccharide binding) fold domains (CHANG ET AL., 2005; MULLEN ET AL., 2005).

Although discovered in a screen for Blm-interacting proteins, Rmi1 and Rmi2 associate more closely with Top3α (SINGH ET AL., 2008); the stable Top3α/Rmi1/Rmi2 complex then interacts with Blm. Reduction of Rmi1 levels causes an approximately two-fold drop in Blm protein levels, and an approximately ten-fold drop in Top3α protein (YIN ET AL., 2005), indicating a role in stabilization of the proteins in the cell. Rmi1 & Rmi2 also appear to be required for Blm localization to sites of DNA damage and for mitotic Blm phosphorylation (SINGH ET AL., 2008).

Disruption of Rmi1 phenocopies mutations in Blm and Top3α, presumably due to their lowered protein levels (as mentioned above). Deletion of yeast Rmi1 resembles deletion of Top3, which could each be partially rescued by Sgs1 (CHANG ET AL., 2005; MULLEN ET AL., 2005). Mice that are homozygous null for Rmi1 result in early embryonic lethality (CHEN ET AL., 2011), resembling the Top3α phenotype. In humans, a genetic

variant of Rmi1 causes increased cancer susceptibility, resembling the phenotype of mutations in Blm (BROBERG ET AL., 2007).

When Rmi1 was added to the Blm-Top3α complex *in vitro*, double Holliday junction dissolution activity was increased several fold (RAYNARD ET AL., 2006; WU ET AL., 2006), indicating a functional aspect to the binding protein. In yeast, this effect appears to be due to Rmi1 stimulating the decatenation activity of Top3 (CEJKA ET AL., 2010). In humans, Rmi1 and Top3α together stimulated the Holliday junction unwinding activity of Blm (BUSSEN ET AL., 2007).

Rmi2 forms a complex with Rmi1 through their OB-folds, rendering it more soluble (XU ET AL., 2008). Unlike Rmi1, however, sequence homology indicates that Rmi2 exists only in vertebrates and plants (XU ET AL., 2008). Intriguingly, the *Drosophila* species do not appear to contain any Rmi homologues.

Gel filtration suggests that the complex exists in a 1:1:1:1 ratio (Blm:Top3α:Rmi1:Rmi2) (XU ET AL., 2008), although the structure of the entire complex is not known. RPA has also been found associating with the complex, which would be expected as it binds Blm and is located at regions of ssDNA (the substrate for Top3α).

1.3.3 The BTR complex is involved in several pathways

Together, the complex of Blm, Top3α, Rmi1 and Rmi2 is termed the "BTR" complex. This stable complex is able to target a unique set of substrates in the cell.

The BTR complex is involved with the Fanconi anemia complex, particularly in the repair of interstrand crosslinks (HEMPHILL ET AL., 2009). A larger complex termed BRAFT contains Blm, RPA, FANC proteins, and Top3α (Table 2). FANCM interacts specifically with Rmi1-Rmi2 to recruit the BTR complex to DNA damage and coordinate it with the Fanconi anemia core complex (DEANS & WEST, 2009).

The BTR complex also localizes to anaphase bridges to assist with chromosome segregation (CHAN ET AL., 2007). This function is especially important in the telomere regions, as these areas are late replicating and their unique structure makes them difficult to replicate (BAREFIELD & KARLSEDER, 2012). These DNA bridge structures may be HJ's or late replicating intermediates, which can be undone by RecQ and Top3 (SUSKI & MARIANS, 2008).

While the BTR complex has many important roles in the cell, several questions about its mechanism remain. Why is Top3β not able to substitute for Top3α? What happens to the structure of the DNA as the Holliday junctions approach each other? At what point in the process is an interaction between the helicase and topoisomerase necessary? How does the complex form so that the active sites are located at the appropriate positions on the substrate? This work advances our understanding of this process by addressing some of these questions.

2. Essential functions of the C-terminal domain of Topoisomerase IIIα in double Holliday junction dissolution

2.1 Introduction

Maintaining genomic stability requires efficient repair of DNA breaks with minimal genetic changes. The complex of Top3α and Blm has been shown to convergently migrate double Holliday junctions (dHJ's), a late intermediate of double-strand break repair, into solely non-crossover products (WU & HICKSON, 2003; PLANK ET AL., 2006). The significance of this antirecombinogenic function can be seen in the phenotype of Blm-deficient cells, which show a marked increase in sister chromatid exchanges (CHAGANTI ET AL., 1974) and loss of heterozygosity (LAROCQUE ET AL., 2011).

Blm and Top3α together are sufficient for dHJ dissolution (WU & HICKSON, 2003; PLANK ET AL., 2006; CEJKA ET AL., 2010), and the two proteins are known to directly interact (WU & HICKSON, 2002). In yeast, the ~100 N-terminal amino acids of Sgs1, the yeast homologue of Blm, are required for interaction with Top3 (BENNETT ET AL., 2000; FRICKE ET AL., 2001). The Top3α-interacting domain of human Blm has also been identified, although some ambiguity remains. Wu *et al.* (2000) showed that both the N- and C-terminal ~200 amino acids of human Blm can independently bind Top3α in a far Western analysis (WU ET AL., 2000). However, Hu *et al.* (2001) showed using co-immunoprecipitation that the N-terminal region is solely responsible for the interaction

(HU ET AL., 2001). Information on the region of Top3α that binds Blm is completely absent.

In addition to Blm and Top3α, the small structural proteins Rmi1 and Rmi2 were found to be stabilizing components of the complex in a variety of organisms (RAYNARD ET AL., 2006; WU ET AL., 2006; SINGH ET AL., 2008; XU ET AL., 2008). The deletion of either Rmi1 or Rmi2 recapitulates the Blm-deficiency hallmark of increased sister chromatid exchanges (YIN ET AL., 2005; XU ET AL., 2008). However, *Drosophila* does not appear to possess any homologues of either structural protein (XU ET AL., 2008).

In metazoans, there exists a pair of type IA topoisomerases: Top3α and Top3β. Although both can perform relaxation *in vitro* on topologically constrained DNA with single-stranded regions (HANAI ET AL., 1996; SEKI ET AL., 1998; GOULAOUIC ET AL., 1999; WILSON ET AL., 2000), Top3β cannot substitute for Top3α in dHJ dissolution (PLANK ET AL., 2006). Their *in vivo* effects are similarly distinct: while Top3α is absolutely essential, Top3β mutants show only a modest reduction in lifespan (LI & WANG, 1998; KWAN & WANG, 2001; PLANK ET AL., 2005), indicating that relaxation activity alone is insufficient for the full range of *in vivo* functions. Since Top3β has no functional interaction with Blm (SEKI ET AL., 2006), the essential function of Top3α may be alongside Blm in the recombinational repair pathway.

Top3α and Top3β share the type IA catalytic domain. The ~600 N-terminal residues of Top3α and Top3β, including the catalytic core and active site tyrosine, are

very similar, with 63% similarity and 43% identity between the human enzymes (57% and 35% in *Drosophila*, respectively). However, the proteins greatly diverge in length and sequence composition of their remaining C-termini (Figure 3A), suggesting a potential region of protein-protein interaction specificity.

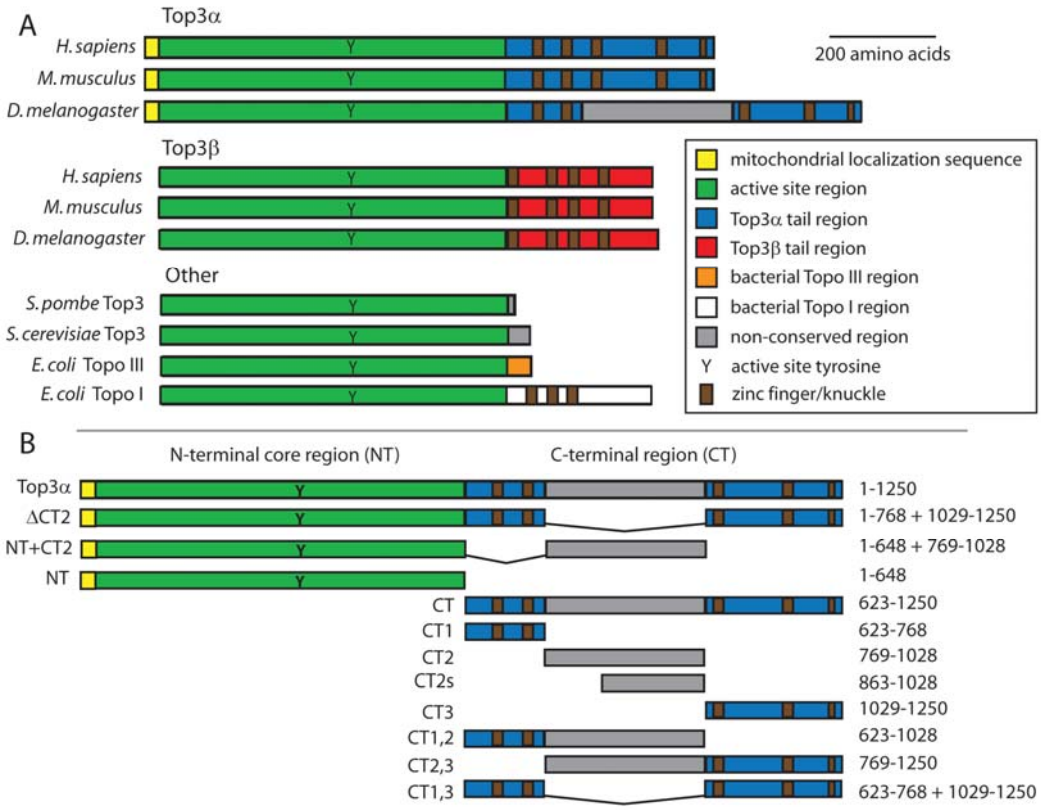

Figure 3: Alignment of the type IA topoisomerase family and constructs of *Drosophila* Top3α used in this study.

A. Alignment of the type IA topoisomerase family. The N-terminal region, including the active site tyrosine (Y), is conserved across all species (green). Among the metazoans, the two isoforms (Top3α and β) are distinguished based on their distinct tail regions (blue and red). Although the tails loosely align across the metazoans, the *Drosophila* Top3α tail contains a unique insert (gray). **B**. Constructs of *Drosophila* Top3α used in this study. The boundaries were based on the alignment in part A. Amino acids included are listed on the right. All constructs were made with an N-terminal GST tag and C-terminal hexahistidine tag (not illustrated).

Here, we show that the unique C-terminus of *Drosophila* Top3α is necessary for the interaction between Blm and Top3α, for dHJ dissolution to occur efficiently, and to rescue the viability of *top3α* null flies. In addition to the conserved Top3α C-terminus, the *Drosophila* enzyme contains an inserted region that can independently bind to Blm, perhaps compensating for the absence of the Rmi structural proteins. Top3α lacking this region can only partially rescue *top3α* null flies. The Top3α C-terminus is also involved in binding to DNA substrates, substantially contributing to the binding activity. Together, these data reveal the essential role for the Top3α C-terminus in recombinational repair.

2.2 Results

2.2.1 The unique C-terminus of Top3α is important for dissolution

Since Top3α and Top3β have distinct cellular and biochemical functions, and the major structural difference resides in their C-termini (Figure 3A), we examined the properties of the Top3α C-terminus. We constructed a series of C-terminal truncation mutants (Figure 3B). The N-terminal 648 amino acid construct (NT) was purified and tested for relaxation activity. Top3α NT was active in relaxing a hypernegatively supercoiled plasmid, with only a slight reduction in specific activity compared to the full-length enzyme (Figure 4A).

We then tested Top3α NT in the dHJ dissolution assay. The dHJ substrate contains two topologically constrained Holliday junctions separated by a homologous

region of 165 base pairs (PLANK ET AL., 2006). Top3α and Blm have previously been shown to dissolve the dHJ substrate into two separate double-stranded DNA circles (PLANK & HSIEH, 2006). At comparable levels of relaxation activity, full-length Top3α shows clear dissolution products, while Top3α NT could only minimally support dHJ substrate dissolution, with a greater than two-fold reduction in dissolution activity (Figure 4B).

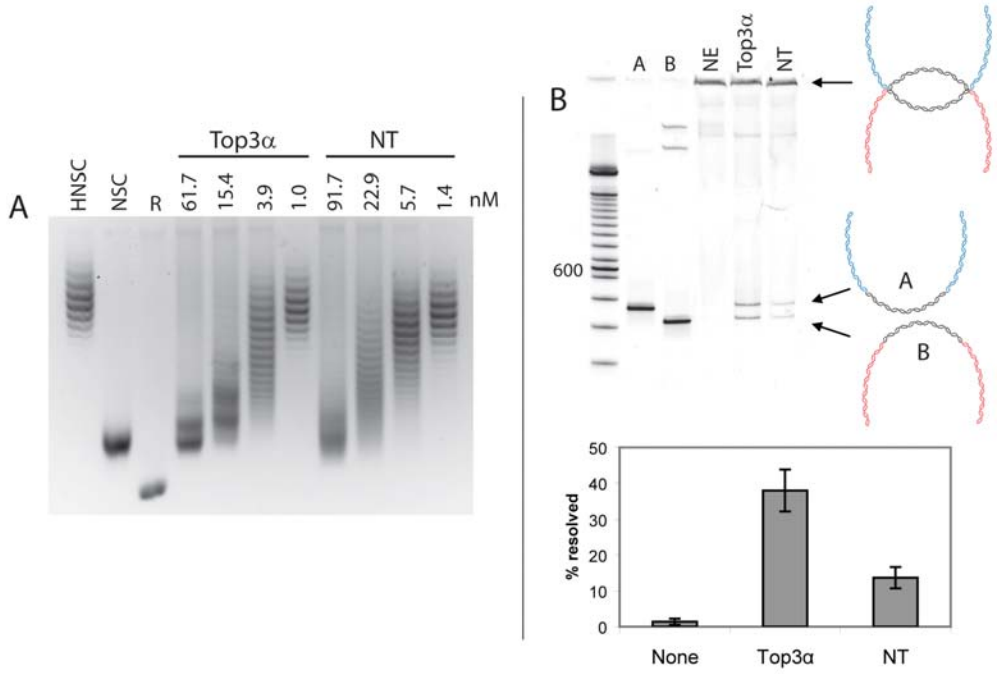

Figure 4: Although Top3α NT is active, dHJ dissolution is compromised.

A. Full-length Top3α and Top3α NT display comparable relaxation activity. Top3α can relax a hyper-negatively supercoiled (HNSC) DNA to the NSC negatively supercoiled (NSC) level, but not to fully relaxed (R). **B.** While full-length Top3α can support dissolution of the dHJ substrate, Top3α NT shows a significant reduction in dissolution activity. NE = no enzyme. Equal activity levels of Top3α & Top3α NT were added. Reactions contain Blm & RPA in addition to the specified topoisomerase. Reaction products were digested with BamHI and run on an acrylamide gel. Diagram of dHJ substrate and reaction products are shown to the side. Reactions are quantified on the chart below from three independent experiments.

2.2.2 RPA stimulates dHJ dissolution and Top3α relaxation

Previously, it has been shown that RPA specifically stimulates the dHJ dissolution reaction (PLANK ET AL., 2006). We tested Top3α NT for stimulation of dissolution by RPA. Although stimulation of the dissolution reaction was seen for both full-length Top3α and Top3α NT, the stimulation increased proportionally to RPA concentration only when full-length enzyme was used (Figure 5). Stimulation using Top3α NT was only observed at a higher level of RPA, and did not continue to increase with RPA concentration.

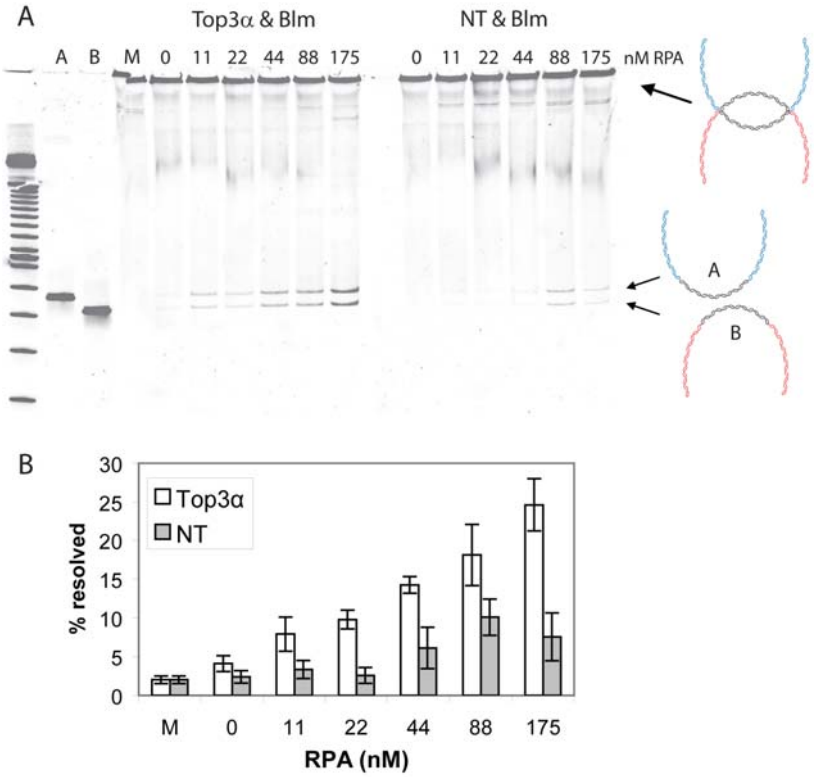

Figure 5: RPA stimulates dHJ dissolution.
Stimulation increases with RPA concentration only when the C-terminus is present (Top3α vs. NT). Data from at least three independent experiments is shown in B.

Although Blm is known to be stimulated by RPA (BROSH ET AL., 2000), it is also possible that Top3α, which requires access to ssDNA, may interact with RPA. To test for this interaction, RPA was added to the relaxation assay for topoisomerase activity. RPA caused a several-fold increase in relaxation activity, whether it was added before or after Top3α, indicating a direct effect (Figure 6A). Surprisingly, RPA was also able to significantly stimulate the activity of Top3α NT (Figure 6B). The T4 phage and yeast equivalents, gp32 and SSB, showed no effect (data not shown).

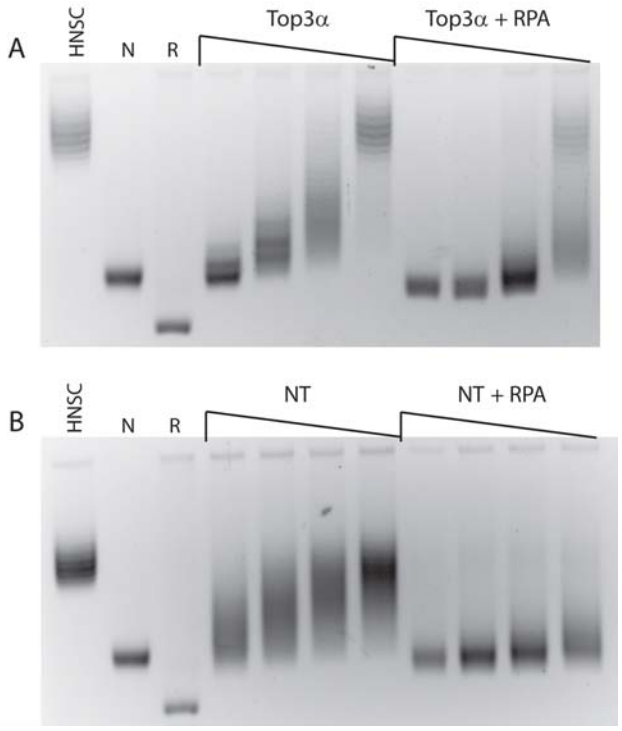

Figure 6: RPA stimulates relaxation activity of both full-length Top3α and Top3α NT. A drastic increase in relaxation activity is evident with both full-length Top3α (A) and Top3α NT (B). Dilutions on the right half of the gel are identical to that on the left, with the addition of 175 nM RPA in each lane.

2.2.3 The Top3α C-terminus is involved in binding Blm

Because dissolution requires coordination with Blm, we tested Top3α NT for the ability to bind Blm. Top3α and Top3α NT with N-terminal glutathione-S-transferase tags were bound to glutathione resin, incubated with nuclear extract or purified Blm, and washed; bound Blm was visualized by Western blot. While bound Blm is clearly evident in the presence of full-length Top3α, Top3α NT shows only minimal binding (Figure 7A&B). The clear difference between the two constructs suggests that the essential role of Top3α C-terminus may be to interact with Blm.

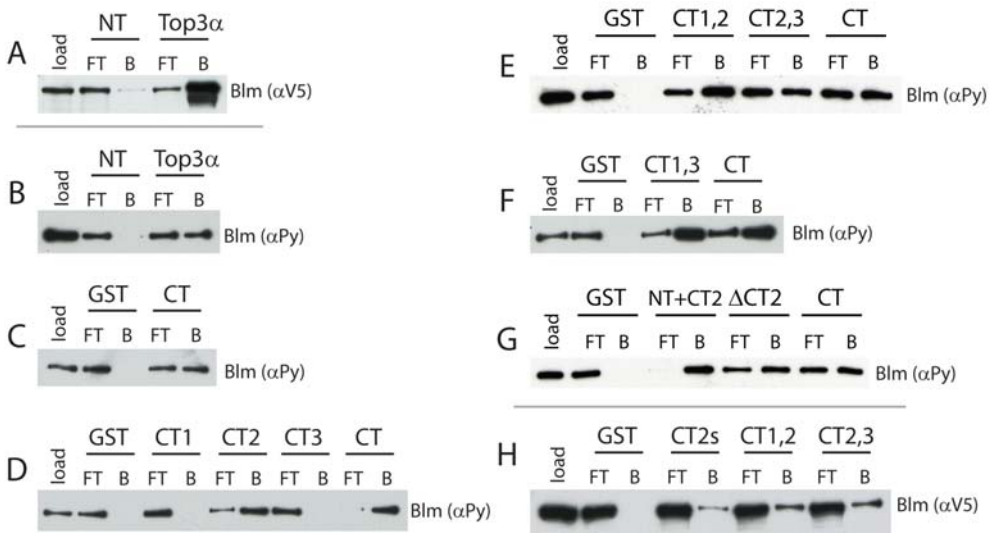

Figure 7: Binding of Blm to various Top3α constructs.

A. Blm binds to full-length Top3α, but barely to NT, in nuclear extracts. **B.** Purified Blm binds to full-length Top3α, but barely binds NT. **C**. Blm binds Top3α CT alone, and does not bind a GST control. **D.** Blm cannot bind CT1 or CT3 alone, but does bind CT2. **E**. Blm binds both CT1,2 & CT2,3. **F.** Blm can bind to covalently connected CT1 and CT3 (CT1,3). **G.** Blm can bind both NT+CT2 and CT2. **H.** Blm can bind to CT2s. *A* & *H* are pulldowns from nuclear extracts and use the V5 antibody. *B-G* use purified Blm and the GluGlu (Py) antibody.

To directly test this hypothesis, Top3α C-terminus (CT) was constructed and purified. Top3α CT was immobilized and incubated with purified Blm as above. In contrast to GST alone, Top3α CT clearly shows retained Blm (Figure 7C). Therefore, Top3α CT is able to independently bind Blm, and presumably contributes this function to the full-length protein.

We made a series of C-terminal sub-domain constructs to narrow down the binding region (Figure 3B). When compared to the other metazoan enzymes, *Drosophila* Top3α contains a unique insert in its C-terminus (Figure 3A). The insert sequence is not homologous to any known protein, and aligns only to the Top3α C-termini of the genus *Drosophila*, among which it is conserved (Figure 8). The first third of the insert is extremely glycine-rich (55%); the remainder is somewhat rich in lysine (8%), but contains no other outstanding features. This insert was used to define the boundaries for dividing the C-terminus: the insert was defined as CT2, while the section prior to it was CT1, and the section following was CT3. Both individual (CT1, CT2, CT3) and overlapping (CT1,2 and 2,3) constructs were made (Figure 3B). When tested individually, only the *Drosophila* unique region, CT2, bound Blm (Figure 7D). This result was surprising given that other species' Top3α are known to interact with Blm. As expected, both CT1,2 and CT2,3 also interact with Blm (Figure 7E).

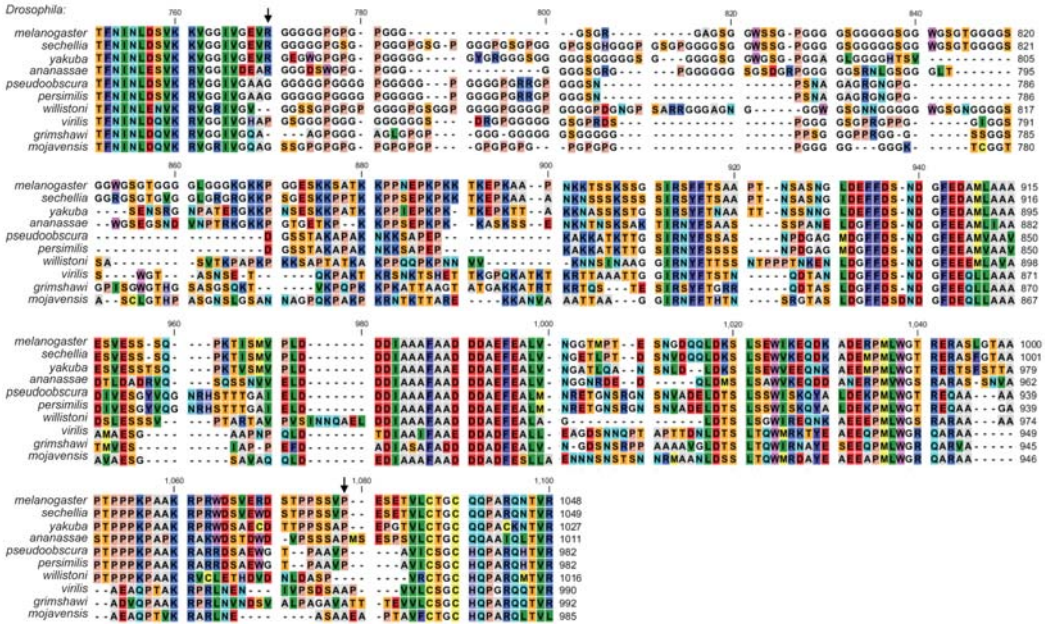

Figure 8: Alignment of CT2 regions across the genus *Drosophila*.
The latter part of the region has highly conserved patches, while the N-terminal amino acids, which are highly glycine-rich, are more variable in length and composition.

To determine if CT2 was necessary, or if the remaining tail was sufficient, we constructed CT1,3, which covalently connects regions 1 and 3. This CT1,3 construct was also able to independently bind to Blm (Figure 7F). Therefore, the *Drosophila* Top3α enzyme appears to contain two regions capable of independently binding Blm: CT2, the insert present only in *Drosophila*, and CT1,3, corresponding to the C-terminus in other metazoans. To verify that the two domains (CT1,3 and CT2) could interact with Blm in the context of the enzyme, we added each back to the core domain, creating Top3α ΔCT2 and NT+CT2. Both constructs were able to interact with Blm (Figure 7G). To confirm that the conserved CT2 area was involved in binding Blm, an additional

construct was made which excluded the glycine-rich portion, dubbed CT2s (for "short"); this construct could still pulldown Blm from a nuclear extract (Figure 7H).

2.2.4 Characterization of Top3α ΔCT2

To investigate the role of CT2 in the context of dHJ dissolution, we assayed the Top3α ΔCT2 construct. This enzyme is more comparable to human Top3α in length and composition (Figure 3). Similar to Top3α NT, the Top3α ΔCT2 was active in relaxation with a specific activity comparable to wildtype (Figure 9A). When added at equal activity, Top3α ΔCT2 was able to support dHJ substrate dissolution similar to wildtype levels (Figure 9B). Therefore, *Drosophila* Top3α ΔCT2 is capable of recapitulating the *in vitro* activity of the full-length enzyme.

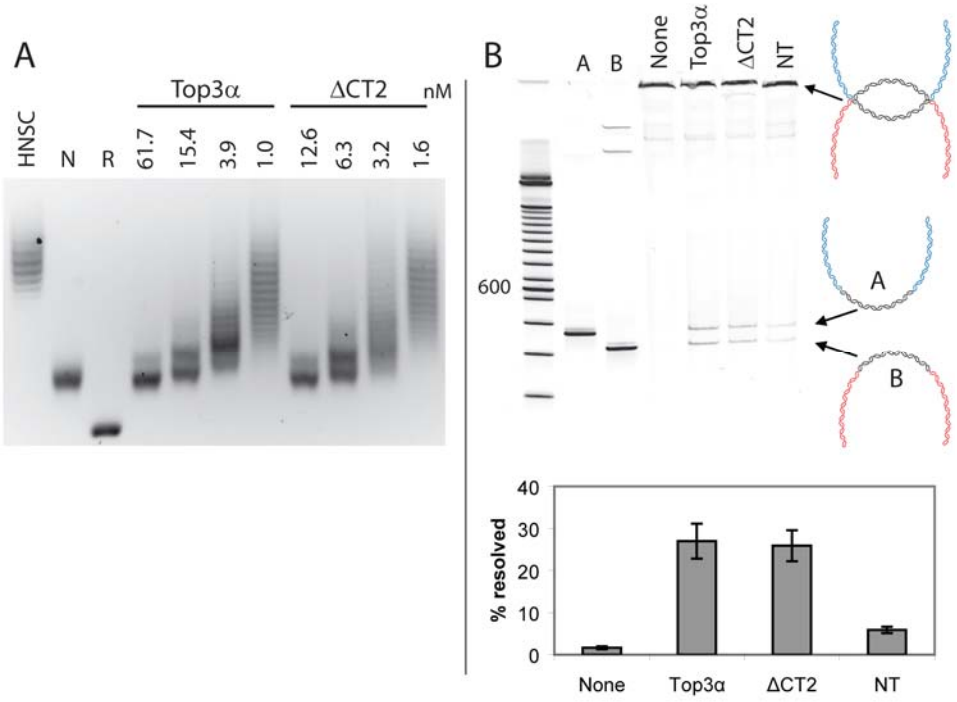

Figure 9: Full-length Top3α and Top3α ΔCT2 show similar levels of activity in relaxation and dHJ substrate dissolution.

A. Top3α can relax a hyper-negatively supercoiled (HNSC) DNA to the NSC negatively supercoiled (NSC) level, but not to fully relaxed (R). **B**. Top3α ΔCT2 is sufficient for dHJ substrate dissolution at wildtype levels. Equal activity levels of Top3α & Top3α ΔCT2 were added. Reactions contain Blm & RPA in addition to the specified topoisomerase. Dissolution reactions were ethanol precipitated and digested with BamHI before being run on an acrylamide gel. Diagram of dHJ substrate and reaction products are shown to right of gel. Reactions from three independent experiments are quantified on the chart below.

2.2.5 The C-terminus is critical in *Drosophila*

Top3α is essential in flies, but can be fully rescued by a transgene expressing a full-length Top3α-YFP construct (WU ET AL., 2010). To test the *in vivo* role of the CT, a Top3αNT-YFP transgene was constructed. A fly line was then generated which contained the top3α^{54} null on the second chromosome opposite a balancer chromosome

(containing wild-type Top3α) and the transgene on the third chromosome opposite a wild-type chromosome (top3α^{54}/SM6; P{Top3αNT-YFP}/+). When this line is crossed *inter se*, the progeny will contain a mix of these possible chromosomes (as outlined in Tables 3 & 4; balancer chromosomes are homozygous lethal). The Top3αNT-YFP construct failed to rescue the viability of the top3α null line, as evident by the complete lack of progeny containing homozygous top3α^{54} mutant (Table 3).

Table 3: The Top3α NT truncation mutant cannot rescue viability of top3α null flies.

The top row lists progeny in the presence of a wildtype copy of Top3α, while the bottom row lists flies with the null mutant (i.e. rescues). Number of flies is shown, with the relative ratio underneath in parentheses. Flies containing the null mutant and the Top3α NT transgene were still inviable, as none were observed. (I created the construct, and the cross was performed by Chung-Hsuan Wu at Academia Sinica.)

		+ / +	NT / +	NT / NT
		0 copies	**1 copy**	**2 copies**
top3α^{54} / Top3α	**wt**	85 (1)	202 (2.4)	78 (0.92)
top3α^{54}/ top3α^{54}	**null**	0 (0)	0 (0)	0 (0)

While CT2 does not appear to be necessary *in vitro*, the region is highly conserved among *Drosophila* species (Figure 8). To determine if CT2 is necessary *in vivo*, a Top3$\alpha\Delta$CT2-YFP transgene was constructed. As above, a line was constructed with the top3α^{54} null mutant on the second chromosome and the transgene on the third chromosome, and mated *inter se*. A low percentage of rescue was seen with the Top3$\alpha\Delta$CT2 construct, as indicated by the few progeny containing both the top3α^{54} null mutant and the transgene (Table 4). Compared to control flies (top row), a single copy of

the Top3α ΔCT2 transgene only rescued ~5% of the homozygous top3α null flies, while two copies rescued ~10%. This low level of rescue efficiency indicates that CT2 has critical *in vivo* functions, although the Top3α ΔCT2 construct still retains partial functionality.

Table 4: Top3α ΔCT2 can partially rescue viability of top3α null flies.

The top row lists flies with a wildtype copy, while the bottom row lists rescues. Number of flies is listed with the relative ratio in parentheses underneath. The top3α null line is inviable (bottom left). In the presence of the mutant, about 5% of flies with one copy and 10% with two copies are able to survive. (Construct created by Jianhong Wu. Cross performed by Chung-Hsuan Wu at Academia Sinica; I also performed this cross with similar results.)

		+ / +	ΔCT2/+	ΔCT2/ΔCT2
		0 copies	**1 copy**	**2 copies**
top3α^{54}/ Top3α	**wt**	568 (1)	1154 (2.0)	556 (0.98)
top3α^{54}/ top3α^{54}	**null**	0 (0)	54 (0.10)	56 (0.10)

To test for fertility defects, flies that were top3α null and contained the Top3α ΔCT2 construct (*i.e.* rescues) were mated to wildtype flies (P2 line) of the opposite sex. Four single copy females were mated to two male P2 flies, and two single copy males were mated with five P2 virgin females. Additionally, five double copy females were mated to one P2 male, and three double copy males were mated to five P2 virgin females. Although the progeny were not counted, all crosses were observed to produce multiple viable offspring. Qualitatively, it was observed that double copy flies, of both genders, produced wildtype levels of offspring, while single copy flies produced fewer (about half).

2.2.6 DNA binding activity of the Top3α CT

Dissolution requires a tripartite complex of Top3α, Blm, and DNA. To determine if Top3α CT contributes to DNA interactions, the Top3α constructs were tested for DNA binding activity using an elecrophoretic mobility shift assay (EMSA) with a series of radiolabeled DNA constructs (Table 5). Full-length Top3α, Top3α NT, and Top3α CT were incubated with single-stranded, double-stranded, and static-X (a non-migratable Holliday junction) DNA, as previously described (CAPP ET AL., 2009). Full-length enzyme showed almost complete binding of all three substrate types (Figure 10A). In contrast, Top3α NT showed very little binding above background, with only the ssDNA showing a significant level of binding. This region of the protein contains the type IA topoisomerase domains I-IV, which are known to interact with ssDNA (CHANGELA ET AL., 2007). Top3α CT showed significant binding on all substrates. Although not equivalent to full-length enzyme, Top3α CT contributes significantly to DNA binding. To test which sub-domains are involved, the various Top3α CT constructs were tested on ssDNA. CT1,3 was the only sub-region able to bind strongly (Figure 10B), indicating that CT1 and CT3 work together.

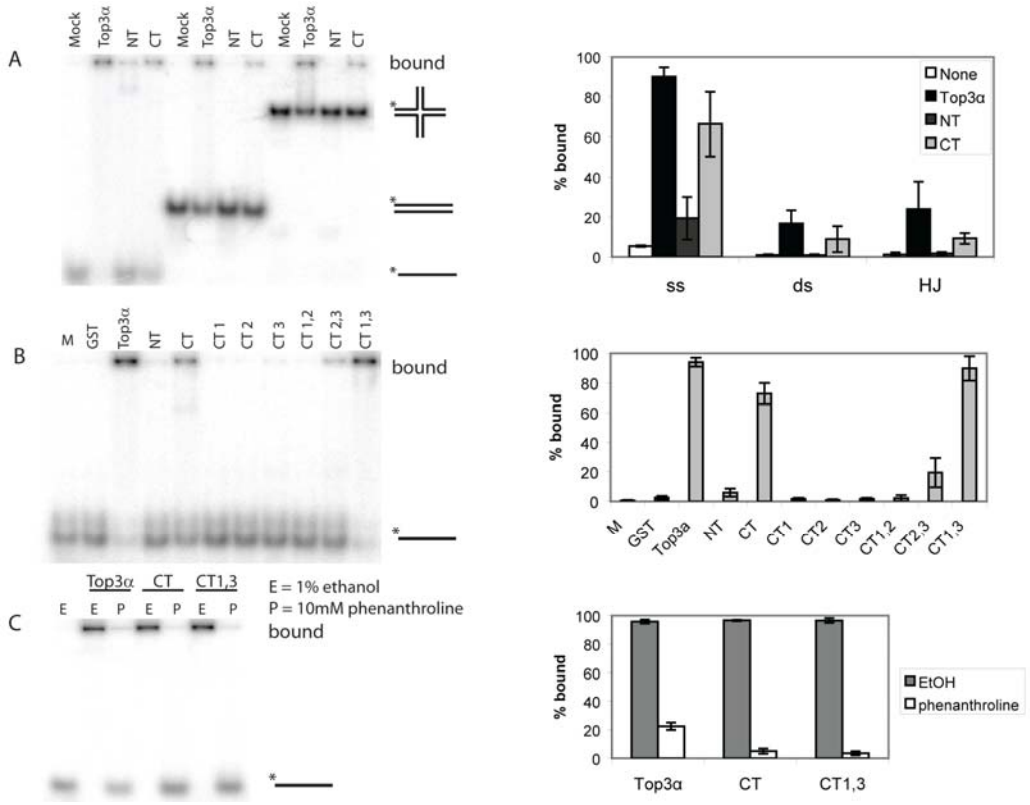

Figure 10: The C-terminus of Top3α is involved in DNA binding.

A. Binding of Top3*α*, Top3*α* NT, and Top3*α* CT to single-stranded, double-stranded, and static-X radiolabeled DNA substrates. The C-terminus of Top3*α* provides the majority of the binding on all types of DNA. Top3*α* prefers ssDNA, which it requires for activity, but also binds the HJ structure. Data from five independent experiments is quantified in the graph on right. **B.** Binding of Top3*α* CT sub-domains to ssDNA. Quantified data from at least three independent experiments is shown in the graph to the right. **C.** Binding of Top3*α*, Top3*α* CT, and CT1,3 in the presence or absence of phenanthroline. Ethanol is used as a control. Binding is abrogated in the presence of phenanthroline. Quantified data from three independent experiments is shown in the graph to the right. M = no protein added.

The Top3*α* CT region contains four putative zinc fingers and a zinc knuckle that could contribute to DNA binding (Figure 3). To test for the importance of the zinc fingers in DNA binding, strong binders were incubated with either 1,10 phenanthroline, which is a zinc chelator, or ethanol (as the phenanthroline is dissolved in ethanol). Full-

length Top3α, Top3α CT, and CT1,3 all showed substantially reduced binding in the presence of the zinc chelator, indicating that the zinc ion is essential for binding (Figure 10C). Full-length Top3α retains some binding, presumably contributed from the active site region (NT), which does not contain zinc fingers and can independently bind ssDNA (Figure 10A). Complete binding of full-length Top3α to ssDNA could be restored by washing away the phenanthroline and adding back zinc (Figure 11). Taken together, these data indicate that the Top3α CT and its zinc fingers are major contributors to DNA binding.

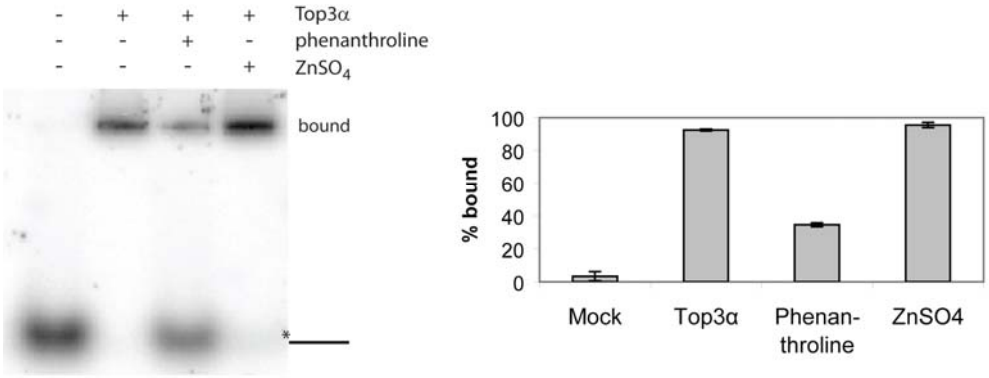

Figure 11: The abrogation of Top3α ssDNA binding by phenanthroline can be restored by adding back zinc.

Immobilized Top3α was incubated with 10 mM phenanthroline. An aliquot was incubated with DNA, and the remaining resin was then washed three times with binding buffer before adding back buffer containing 5 μM ZnSO4. An aliquot was again taken and incubated with labeled ssDNA. By removing the phenanthroline and adding zinc, binding is restored.

2.3 Discussion

Despite possessing seemingly identical relaxation activity, Top3β cannot substitute for Top3α *in vivo* (LI & WANG, 1998; SEKI ET AL., 2006) or in dHJ dissolution (PLANK ET AL., 2006). The main structural difference between the two isozymes lies in their C-termini. Therefore, we investigated the necessity and function of the *Drosophila* Top3α C-terminus.

Relaxation activity of Top3α NT, which truncated the C-terminus, was not significantly altered. However, dissolution of the dHJ substrate, a model recombination intermediate, was greatly reduced. Top3α NT was unable to directly interact with Blm, while Top3α CT could, indicating that the Top3α CT provides a necessary platform for protein-protein interaction. Top3α CT is also involved in the stimulation of dissolution activity by RPA, as truncated enzyme did not display proportional stimulation. However, the Top3α CT was not necessary for RPA to stimulate Top3α relaxation activity. The stimulation of dHJ dissolution by RPA could therefore be related to the interaction with Blm, as Blm and RPA are known to directly interact (BROSH ET AL., 2000) and Top3α CT provides the interaction with Blm.

The *Drosophila* Top3α CT contains an insert that is not homologous to the tails of other metazoans. This insert was used to divide the *Drosophila* Top3α CT for further study. The insert was dubbed CT2, and the divided pieces were CT1 and CT3. CT1,3, which directly connects sections CT1 and CT3, is most homologous to the Top3α CT

domain of other metazoans. CT1,3 is capable of binding Blm, which is consistent with the notion that Top3α from other species can interact with Blm. However, CT2 is also able to independently bind Blm. This insert may be stabilizing the Top3α-Blm complex in place of Rmi1 and Rmi2, structural proteins found in the complex in other species, which have so far not been found in *Drosophila*. In the species we studied, possession of CT2 consistently corresponds with a lack of Rmi proteins. Although CT1,3 and CT2 each had Blm binding activity, the sections CT1 and CT3 individually showed little activity in binding Blm or DNA. It is likely that sections CT1 and CT3 come together three-dimensionally to form a proper scaffold for binding. However, future studies are needed to determine the structural conformation of this region.

The *Drosophila* Top3α ΔCT2, which contains both the enzyme active site and the conserved CT1,3 binding region, is capable of performing dHJ dissolution at levels equal to the wildtype enzyme, indicating that CT2 is not required for dHJ dissolution *in vitro*. This mutant closely resembles the human and other metazoan Topo IIIα enzymes, and therefore the ability to perform dHJ dissolution is not unexpected. However, CT2 contains important *in vivo* functions, which are not apparent in our *in vitro* assays. When the Top3α ΔCT2 mutant is inserted into flies, it is only able to partially rescue *top3α* null flies, and rescuing ability is correlated with the gene copy number of Top3α ΔCT2. As *Drosophila* appear to lack the structural proteins Rmi1 and Rmi2, this insert may be contributing to complex stabilization of Blm-Top3α.

The Top3α CT also plays an extensive role in binding to DNA substrates. Although the catalytic core binds ssDNA as part of its activity, the majority of the observed ssDNA binding of the enzyme was due to the Top3α CT. The tail region also contributed the majority of the binding for double-stranded and static-X substrates. Top3α CT is expected to bind DNA due to its putative zinc fingers, which align with those of other metazoans. When all zinc fingers were present, as in CT1,3, they were able to provide significant binding. Addition of a zinc chelator significantly reduced this binding activity, indicating that the protein is coordinating zinc ions to bind DNA substrates.

Recently, two models have been proposed for the molecular process of dHJ dissolution (PLANK & HSIEH, 2009) (Figure 24). The Unravel & Unlink model proposes a sequential reaction, in which a region of ssDNA is first created between the junctions, followed by coordinated separation of the strands and renaturation. In the HJ Convergent Migration model, the two enzymes are arranged in a complex such that Topo IIIα is able to perform strand passage concomitant with the helicase migrating the junctions. Both models require concerted activity of the two enzymes. Our data reinforce the idea that the two proteins need to be coordinated for dissolution to occur. In the absence of interaction, only limited dissolution occurs. Because some limited dissolution is possible when RPA is present but Blm interaction is limited or missing (as with Topo IIIα NT), this may indicate that the functions of the two enzymes may be separated, as in

the Unravel & Unlink model. In this situation, Blm may be acting first to unwind the intervening strands, which are then held in the melted state by RPA until the topoisomerase can bind and act. This would explain why dHJ dissolution with Topo IIIα NT is not above background in the absence of RPA (see Figure 5B). It is also possible that the optimal situation (when full-length topoisomerase is present) is closer to the HJ Convergent Migration model, with the Unravel & Unlink occurring only under suboptimal situations. Further study will be needed to distinguish the exact mode of action of the complex.

Taken together, the C-terminus of Top3α appears to provide an important interface for protein-protein and protein-DNA interactions. These interactions are critical for the *in vitro* biochemical reactions, including dissolution of dHJs, as well as the *in vivo* functions of the enzyme.

2.4 Experimental Procedures

2.4.1 Purification of Top3α, Top3α NT, Top3α ΔCT2, and NT+CT2

Top3α, Top3α NT, Top3α ΔCT2, and Top3α NT+CT2 were expressed and purified using the baculovirus system in Sf9 insect cells, as in Plank *et al*., 2005 (PLANK ET AL., 2005), with the following exceptions. Cells expressing the mutant proteins (Top3α NT, Top3α ΔCT2, and Top3α NT+CT2) were resuspended in 20 mM Tris pH 8.0, 20 mM KCl, 2 mM MgAC, 3 mM $CaCl_2$, 25% glycerol, and 0.5% NP-40. After douncing, NaCl was added to 350 mM. The solution was incubated on ice for 30 min to precipitate DNA,

then centrifuged at 20,000x*g* for 20 min. Supernatant was loaded onto glutathione resin and purification continued as previously described.

2.4.2 Purification of Top3α CT and CT domains

The Top3*α* CT and CT pieces were expressed in BL21(DE3)pLysS cells. Cells were grown at 37°C for 2 hours, then induced with 1 mM IPTG and grown for 6 hours at 30°C. Cells were then pelleted and frozen. The following steps were performed at 4°C, and all buffers contained 1:1000 Protease Inhibitor Cocktail (Sigma), 20 μg/mL leupeptin, 5 mM 2-mercaptoethanol (IMAC Wash and Elution buffers contained 2.5 mM 2-mercaptoethanol). Pellets were resuspended in 50 mM Tris pH 7.9, 10 mM imidazole, 100 mM NaCl, 10% glycerol, and the solution was sonicated to break open cells. The lysed cells were spun down at 10,000x*g* for 25 min. The supernatant was then incubated with nickel metal affinity resin (Qiagen) for 1 hour. Resin was washed with 10 volumes of 50 mM Tris pH 7.9, 10 mM imidazole, 1M NaCl, 10% glycerol, 0.02% Triton X-100 followed by 50 mM Tris pH 7.9, 10 mM imidazole, 150 mM NaCl, 10% glycerol, 0.02% Triton X-100. Protein was eluted off the resin using 50 mM Tris pH 7.9, 200 mM imidazole, 150 mM NaCl, 10% glycerol, 0.02% Triton X-100 in one column volume aliquots. Peak fractions were determined by Bradford assay (BioRad), pooled, diluted 5-fold with 50 mM Tris pH 7.0, 150 mM NaCl, 10% glycerol, 0.02% Triton X-100, and applied to glutathione Sepharose resin (GE Healthcare). Glutathione resin was washed with 50 mM Tris pH 7.0, 1M NaCl, 10% glycerol, 0.02% Triton X-100 followed by 50 mM

Tris pH 7.0, 150 mM NaCl, 10% glycerol, 0.02% Triton X-100. Protein was eluted by incubation with 50 mM Tris pH 7.9, 150 mM NaCl, 10% glycerol, 10 mM glutathione overnight, followed by dialysis into 20 mM Tris pH 7.5, 150 mM NaCl, 50% glycerol.

2.4.3 Purification of Blm

Recombinant Blm was purified as in Weinert & Rio, 2007 (WEINERT & RIO, 2007), with the following exceptions. All listed steps are at 4°C, and all buffers contain 5 mM 2-mercaptoethanol, 1 mM benzamidine, and 0.1 mM PMSF. The nuclear pellet was resuspended in a DNA precipitation buffer (15 mM Hepes-KOH pH 7.6, 400 mM KCl, 5 mM $MgCl_2$, 1 mM EDTA, 1 mM EGTA) and gently homogenized. This solution was allowed to incubate for 30 min before centrifugation at 20,000x*g* for 20 min. The supernatant was recovered, and 1/10 volume of saturated $(NH_4)_2SO_4$ was then added. Ammonium sulfate precipitation and storage proceeded as above. Precipitates were resuspended in 10 mL ssDNA wash buffer (20 mM Tris pH 7.9, 200 mM NaCl, 10% glycerol, 0.02% Triton X-100) and dialyzed into 2L of this buffer for 2 hours twice. The dialyzed solution was then incubated with 2-3 mL of ssDNA cellulose resin (USB) for 30 min. Resin was washed with wash buffer for 10 min, then incubated with ssDNA elution buffer (20 mM Tris pH 7.9, 1M NaCl, 10% glycerol, 0.02% Triton X-100) for 30 min. Eluate was dialyzed into IP buffer (20 mM Tris pH 7.5, 500 mM NaCl, 10% glycerol, 0.02% Triton X-100) of 1L for one hour, twice, then incubated with 100 μL GluGlu antibody resin (Covance) overnight. Resin was washed and eluted as previously

described. BSA was added to the eluate to a concentration of 0.25 mg/mL; eluate was then dialyzed into storage buffer (40 mM Tris pH 7.5, 150 mM NaCl, 50% glycerol) for three hours, flash frozen, and stored at -80°C.

2.4.4 Hyper-negatively supercoiled plasmid substrate

Hyper-negatively supercoiled plasmid substrate was prepared as previously described (WILSON ET AL., 2000). The plasmid pDHJS AN+ (PLANK & HSIEH, 2006) was used with an ethidium bromide:DNA ratio of 12μg:100ng.

2.4.5 Relaxation activity assay

Activity assays were similar to previous study (PLANK ET AL., 2005). Relaxation activity reactions contained 20 mM Hepes pH 7.6, 1 mM $MgCl_2$, 100 mM NaAc, 1 mM DTT, 0.1 mM EDTA, and 50 ng/μl DNA. Where indicated, 200nM RPA was included. Reactions proceeded at 37°C for 30 min, and were stopped by the addition of NaCl to 600 mM. After 5 min, loading dye and proteinase K (to 50 ng/μl) were added. After a 30 min incubation at 37°C, samples were loaded onto a 1.5% TAE agarose gel containing 0.5 ng/μl ethidium bromide and run at 50V overnight. Gels were destained prior to imaging.

2.4.6 Creation of the dHJ substrate

The dHJ substrate was made as described in Plank *et al*., 2006 (PLANK & HSIEH, 2006), with the following exceptions. Cre reaction buffer was 20 mM Tris, 300 mM LiCl, 1 mM EDTA, pH 8.2. Rather than electroelution, Cre reaction products were gel

extracted and allowed to diffuse overnight into 10x volume of MEN buffer (50 mM MOPS pH 7.0, 10 mM EDTA pH 8.0, 750 mM NaCl), then recovered through a DEAE column (Qiagen).

2.4.7 dHJ substrate dissolution assay

Dissolution of the dHJ substrate was performed as described in Plank *et al*., 2006 (PLANK ET AL., 2006) with the following exceptions. Reactions were incubated at 30°C for 30 min, and contained 15 nM Top3α (25 nM Top3α NT or 20 nM Top3α ΔCT2) and 18 nM Blm.

2.4.8 Protein binding assay

Top3α and its derivatives were bound to glutathione Sepharose resin (GE Healthcare). Equivalent amounts of bound protein were incubated with purified Blm for 30 min at 4˚C in 40 mM Tris pH 7.5, 100 mM NaCl, 4 mM $MgCl_2$, 10% glycerol. The Top3α/NT experiment included 5 μg/mL ethidium bromide. After incubation, resin was watched three times with several volumes of the same buffer. Flow-through and resin samples were run on a 4-20% Criterion acrylamide gel (BioRad), transferred to nitrocellulose, and blotted with mouse anti-GluGlu antibody (Covance). The blot was incubated with HRP-conjugated goat anti-mouse antibody and substrate (Thermo Scientific), and visualized with film (Kodak).

2.4.9 *Drosophila* crosses

The Top3α NT and Top3α ΔCT2 transgenes were generated from the Top3α-YFP transgene (WU ET AL., 2010), by excising the appropriate tail regions and adding back the nuclear localization sequence (amino acids 845-862) between the Top3α and YFP sequences. The transgenes were injected into fly larvae at the Duke Model System Genomics facility. These flies were mated to the homozygous lethal top3α^{54} line to create top3α^{54}/CyO;NT/+ and top3α^{54}/CyO;ΔCT2/+. Each line was mated *inter se*, and the progeny phenotyped and counted to determine rescue efficiency.

2.4.10 DNA binding assay

Oligonucleotides were radiolabeled with ATP[γP^{32}] (Perkin Elmer) using T4 polynucleotide kinase (NEB). Oligonucleotides were purchased from IDT (Table 5). Where required, oligonucleotides were annealed at a 1:3 hot:cold ratio by temperature gradient in a thermocycler. Substrates were subsequently run on an 8% TBE polyacrylamide gel, excised, and electroeluted. Labeled DNA (0.25 nM) was incubated with 30 nM of protein in 40 mM Tris pH 7.5, 50 mM NaAc, 4 mM $MgCl_2$, 1 mg/mL BSA, 10 mM DTT for 30 min at 4°C. Loading buffer was added, and samples were run on an 8% TBE polyacrylamide gel overnight at 4°C. The gel was exposed to a phosphorimager screen and scanned using a Storm scanner.

Table 5: Oligonucleotides used to create DNA substrates.

Each is 60 nucleotides long; the arms of the static-X are 30 base pairs each. Substrates and their components are diagrammed below.

ID	Sequence
7	CGA AGG CCA TGA TTG CGC ACT GAA TAC ATC CTG CCC TGT TAT TAA TTA CGT TAT CTT ACG
8	GTG TTG CCG TCT ACA TGC TTG ATT ATT CTC GAT GTA TTC AGT GCG CAA TCA TGG CCT TCG
9	CGT AAG ATA ACG TAA TTA ATA ACA GGG CAG GAT GTA TTC AGT GCG CAA TCA TGG CCT TCG
11	GCT ACT ACT TCA CTA TCT CGC CGA TCA ACC GAG AAT AAT CAA GCA TGT AGA CGG CAA CAC
12	CGT AAG ATA ACG TAA TTA ATA ACA GGG CAG GGT TGA TCG GCG AGA TAG TGA AGT AGT AGC

Substrate	Description	Components
	ssDNA	7
	dsDNA	7 & 9
	HJ (static-X)	7, 8, 11, & 12

3. Improved methods for constructing Holliday junction substrates

3.1 Introduction

Homologous recombination is an important process in the cell for replication fork recovery, double-strand break repair, and meiotic crossovers (SAN FILIPPO ET AL., 2008). The Szostak model of homologous recombination proposes a double Holliday junction intermediate following strand invasion (SZOSTAK ET AL., 1983), and such junction structures have been observed in yeast (BZYMEK ET AL., 2010). Several studies have shown that the complete absence of Holliday junction processing enzymes results in lethality (ANDERSEN ET AL., 2011; WECHSLER ET AL., 2011). Although most studies use oligonucleotide-based Holliday junction substrates, these short, often immobile structures do not accurately represent the late-stage recombination intermediate.

We previously published a method for creating a novel DNA substrate, the double Holliday junction (dHJ) substrate (PLANK & HSIEH, 2006). This substrate contains two Holliday junctions that are mobile, topologically constrained, and separated by a distance comparable to conversion tract lengths (BLANTON ET AL., 2005; LAROCQUE & JASIN, 2010). The dHJ substrate has been used to characterize the *Drosophila* dissolution complex (PLANK ET AL., 2006; CHEN ET AL., 2012). However, the difficulty of producing the substrate has hindered its use in the field. In this work, we describe new methodology for creating HJ substrates. A helper plasmid that allows constitutive expression of the desired single-strand DNA (ssDNA) streamlines production of the

essential starting material. These ssDNA circles can be used to make single, double, or quadruple HJ substrates. In addition to previously described substrates (containing single and double HJ's), replacing the Cre/lox recombination system with the unidirectional ϕC31 Integrase system increases DNA yield and creates a quadruple HJ substrate that can be dissolved in the same manner as the original dHJ substrate.

3.2 Results

3.2.1 Production of ssDNA

Before the substrates can be constructed, large quantities of ssDNA must be produced (Figure 12, I to II). Previously, the M13K07 helper phage was employed, requiring large quantities of helper phage to first be produced and titered. The pM13g helper plasmid contains the components of the viral coat proteins normally expressed by the helper phage. Cells containing pM13g and a plasmid with the f1 origin constitutively produce phage containing ssDNA from the inserted plasmid.

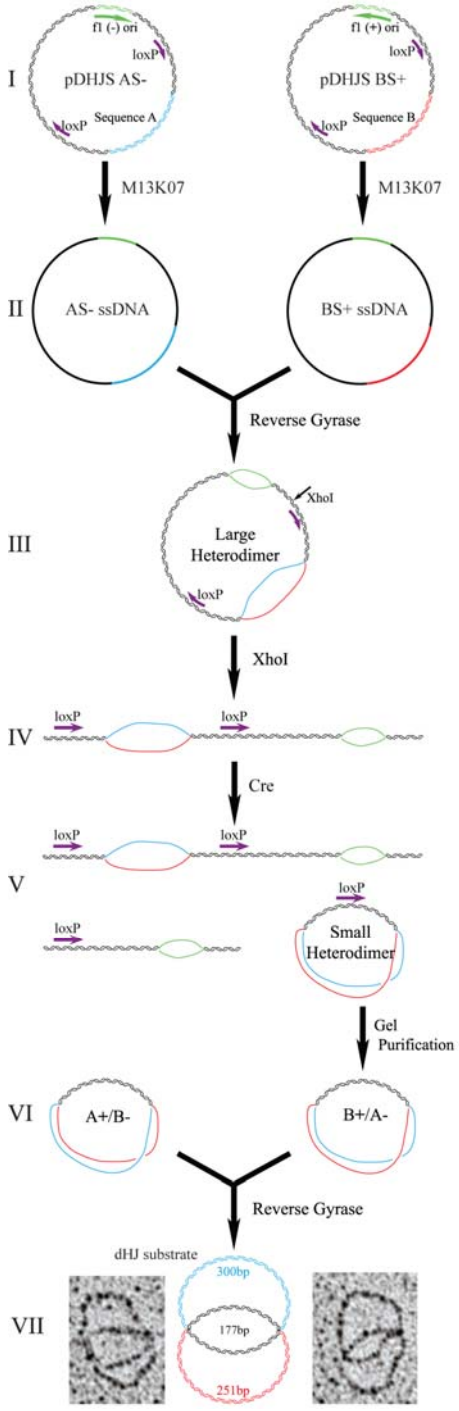

Figure 12: Original method for creating the dHJ substrate.

Outline of the steps involved in creating the original dHJ substrate, as published (PLANK & HSIEH, 2006). Electron microscope images of the final product are included.

To produce ssDNA for the substrates, DH5α cells were transformed with pM13g and made chemically competent (using a standard calcium chloride protocol). These competent cells were then transformed with each of the pDHJS plasmids (modified as described below). Although a strand bias was observed, in that less DNA was made from the (+) plasmids, sufficient DNA could be obtained from large-scale overnight growths. Single colonies were inoculated into 10 mL of Terrific Broth (containing chloramphenicol and gentamicin) and grown for 10-12 hours, so that the cultures were visibly growing but remained in log phase. These cultures were then used to inoculate 2-3 L of Terrific Broth for the large-scale growth.

3.2.2 Gel extraction by diffusion

The largest source of DNA loss during the procedure is the gel extraction step (Figure 12, V to VI). Although we have tried a variety of methods, including electroelution, DEAE paper, Qiagen kits, and beta-agarase, the best yield came from simply chopping up the gel slice and incubating with rotation overnight in buffer (50 mM MOPS pH 7.0, 10 mM EDTA, 750 mM NaCl). The buffer was then separated from the gel by filtration through Kimwipes, and the DNA was recovered and concentrated using a DEAE column (Qiagen).

3.2.3 Single migratable HJ's can be produced

The previously described "DHJS-2" substrate (WEBB ET AL., 2007), which produces two kinds of migratable single Holliday junctions, can also be produced from

the same starting plasmids (Figure 13A). This method uses the same single-stranded DNA and does not require the recombination system. Following annealing with Reverse Gyrase, the substrate can be stored as a stable, large heterodimer.

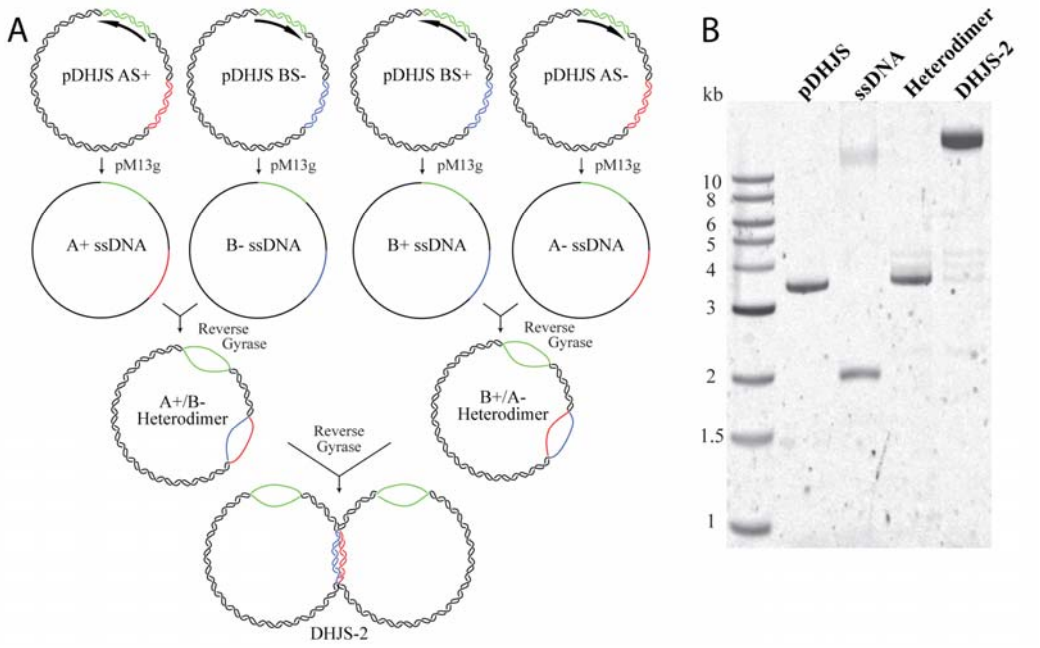

Figure 13: Method for creating DHJS-2.

A. Outline of the steps for producing the DHJS-2 substrate. This method is as published, with the exception of the use of pM13g to create the ssDNA and the presence of the attB/attP sites in the plasmids (which are not used). **B**. Gel electrophoresis of DNA in (A).

Prior to use in a reaction, digestion with BamHI and AlwNI produces two substrates each containing a single migratable HJ (Figure 14A). To ensure that the substrate produced from the updated plasmids maintains activity, DHJS-2-ϕC31 was tested with UvsW as in previous work (WEBB ET AL., 2007). As expected, UvsW is able to migrate the junctions into their products (Figure 14B). Incubating the substrate at 37°C for one hour (heat) is also sufficient to create products.

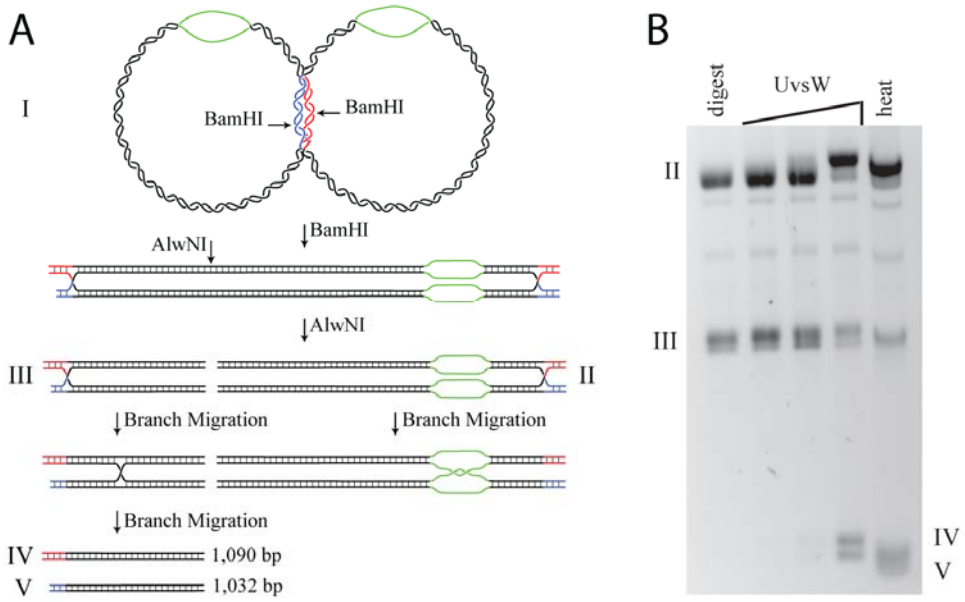

Figure 14: DHJS-2 digestion and migration.

A. Outline of products created by digestion of the DHJS-2. Digestion with BamHI and AlwNI creates two substrates containing single HJ's (II & III). The smaller substrate (III) will migrate into two smaller duplex pieces, while the larger HJ substrate (II) will migrate and be trapped in the bubble region. (Because the red and blue regions are non-homologous, branch migration cannot occur in this direction.) **B**. Products shown on a gel. HJ's can be migrated by heat or the phage T4 enzyme UvsW (WEBB ET AL., 2007).

To observe the substrate and its derivatives, we employed electron microscopy. The substrates were pre-incubated with the ssDNA binding protein gp32 to highlight the ssDNA bubbles. The substrates were then spread onto carbon-coated grids and shadowed with tungsten.

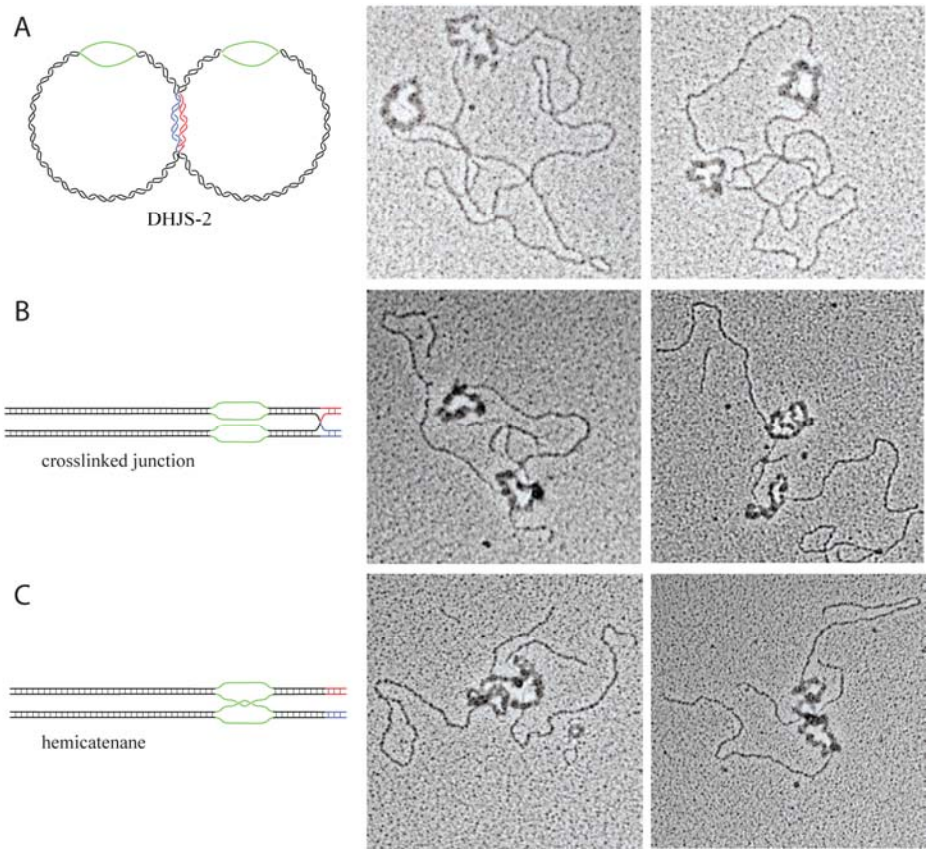

Figure 15: Electron microscopic images of DHJS-2 and derivatives.

DHJS-2 and its derivatives were incubated with gp32 to highlight the single-stranded regions and visualized on an electron microscope. **A**. Undigested DHJS-2. **B**. DHJS-2 crosslinked with psoralen prior to digestion to trap the HJ. **C**. Digested and migrated DHJS-2, which creates a hemicatenane in the bubble region.

The plasmid region of the substrate is very flexible, so the junction region is unclear in the starting molecules, but a molecule containing two origins is evident (Figure 15A). To capture the digested, un-migrated HJ, the DHJS-2 was crosslinked with psoralen prior to digestion. On these molecules, a 4-way junction is clearly evident on the small arms extending from the origin bubble (Figure 15B). Molecules that have been

digested but not crosslinked show a connection at their bubble regions (Figure 15C). These images verify our expectations of the substrate conformation.

3.2.4 Replacing the recombination system

The Cre recombinase reaction is bidirectional, meaning that a maximum of 50% of the product is created (Figure 12, IV to V). Transition of the system to the unidirectional ϕC31 integrase theoretically allows 100% recombination, meaning that all of the DNA molecules put into the reaction contributes useable product for the downstream reactions.

To convert the dHJ substrate to the ϕC31 integrase system, the two loxP sites in the starting plasmids were replaced with sequential attB and attP sites. These unique sites become attL and attR following recombination, effectively preventing the reverse reaction (Figure 16, IV to V). Oligonucleotides containing the sequences were obtained and annealed to make DNA duplex with sticky ends, which were then ligated into each of the digested plasmids (see Experimental Procedures). Using this system, we regularly observe 90% recombination.

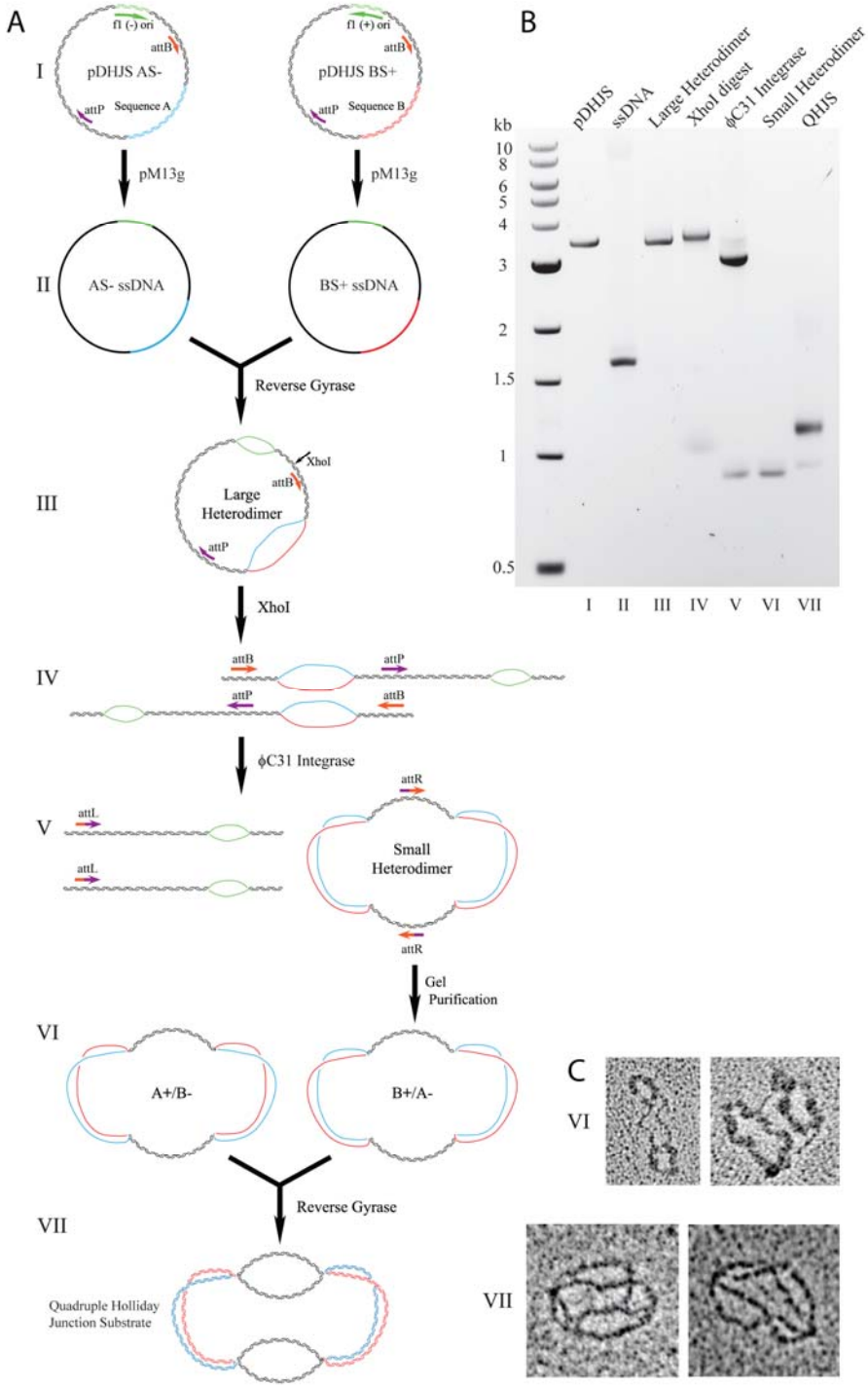

Figure 16: Method for creating the quadruple HJ substrate.

A. Outline of creation of the quadruple HJ substrate, using the ϕC31 Integrase system. **B**. Products from (A) on an agarose gel. **C**. Electron microscope images of VI & VII.

Surprisingly, despite using a dilute DNA solution (that allowed solely intramolecular reactions with Cre recombinase), ϕC31 Integrase produced almost exclusively dimer products (Figure 16A, IV to V, & B, lane 6). Although a mix of monomers and dimers can be produced when using the starting plasmids, using the large heterodimer as a substrate produce only dimers, and occasionally tetramers (data not shown). Visualization by electron microscopy (Figure 16C) and reaction with Top2 (data not shown) confirmed that the dimers were produced via recombination rather than catenation, and that the final product contains four Holliday junctions.

3.2.5 The quadruple HJ substrate can be dissolved by the Blm-Top3α complex

A hallmark of the dHJ substrate is its ability to be dissolved by Blm and Top3α (PLANK ET AL., 2006; CHEN ET AL., 2012). To ensure that the new version of the substrate maintains functionality, we performed the dissolution reaction using the *Drosophila* Blm-Top3α complex. As with the original dHJ substrate, Blm, Top3α, and ATP were all required for substrate dissolution (Figure 17). We observed levels of dissolution comparable to that of the previous substrate (~30%) (compare with Figure 4).

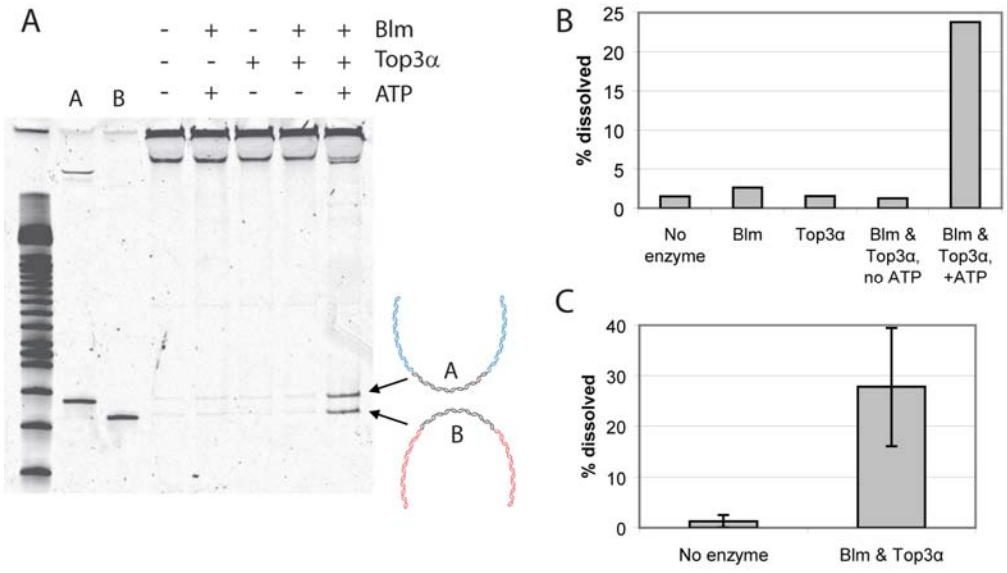

Figure 17: Dissolution of the quadruple HJ substrate.

A. Dissolution of the quadruple HJ substrate requires Blm, Top3α, and ATP, as with the dHJ substrate (PLANK ET AL., 2006). Substrates were digested with BamHI after reaction, prior to being run on an acrylamide gel. **B**. Quantification of (A). **C**. Quantification of the amount of dissolution achievable with the quadruple HJ substrate. (n=3)

3.3 Discussion

In updating the dHJ substrate method, we sought to make the process less labor-intensive and more efficient. The two points we focused on were production of single-stranded DNA and the recombination reaction.

Previously, production of the ssDNA required preparation of large quantities of the M13K07 phagemid and performing phage titration. In addition, the pDHJS plasmids must be freshly transformed into phage-competent (F') cells, and colonies tested for their response to the addition of phagemid. In the updated system, the pDHJS plasmids are transformed into cells containing the pM13g plasmid, and phage is constitutively

expressed. The best expression results were obtained from freshly transformed cells, but there was little variation among colonies, preventing the need to test colonies prior to scaling up. Once the competent cells are produced, production of the ssDNA requires minimal attention.

Gel extraction is always the largest source of DNA loss during the procedure. Although we have tried a variety of methods, the greatest return was when the gel slices were finely chopped, incubated in buffer overnight, and recovered through a DEAE column, similar to the method commonly used to recover PAGE-purified oligonucleotides.

Another significant source of DNA loss is the Cre recombination step. The loxP sites that are the substrates for Cre remain intact following recombination, so the products can also become substrates. Due to the bidirectionality of the Cre reaction, a maximum of 50% of the DNA is in product form. In large scale reactions, 20-40% is much more common, meaning that up to 80% of the initial DNA is not used for further substrate preparation. In contrast, the distinct attB and attP sites, which are the substrates for ϕC31 integrase, recombine to form attL and attR, making the system unidirectional. Product formation, even in large scale reactions, was regularly 90%, reducing the loss of DNA by five-fold.

The components of the dHJ substrate can also be used to create the DHJS-2, which can be digested to make two migratable single Holliday junctions. Due to the

ability of the junctions to spontaneously migrate, it is important to use the highest concentration of magnesium and the lowest temperature and incubation time possible for the enzyme in question. Reactions should also be stopped with magnesium and ethidium bromide to prevent further migration. Alternatively, thermal branch migration of the substrate will create a hemicatenane structure that can be used for decatenation studies (Figure 14, II).

While the original dHJ substrate was extensively characterized to prove the existence of Holliday junctions, an additional method is to directly visualize the DNA. Images of the original dHJ substrate show two clear junctions connecting the circles of different sizes (Figure 12, VII). The new ϕC31 substrate clearly shows four Holliday junctions with the appropriate size arms connecting them (Figure 16C). Subsequent assays revealed that linearized plasmids could form monomer and dimer products, but heterodimers (containing a large single-stranded bubble region adjacent to the recombination sites) were unable to form monomer products (data not shown). Therefore, the character of the local DNA affects the ϕC31 recombination reaction and led to the formation of dimer product at the small heterodimer stage (Figure 16A, V). While entirely unexpected, the quadruple HJ product can be produced more efficiently and is equally capable of modeling dHJ dissolution *in vitro*.

Similarly, the expected conformations of DHJS-2 and its derivatives were clearly visualized (Figure 15). Molecules containing two origin regions that produce HJ's or

hemicatenanes, depending on the conditions, were evident. This substrate is very easy to produce efficiently, as no recombination step is necessary, and should be useful for future studies of HJ migration or decatenation. Recent studies of decatenation have utilized interlocked, ssDNA circles (YANG ET AL., 2010), which are unlikely to be present inside the cell. The catenated bubbles in the context of a duplex provides a more physiological substrate to study the same reactions.

3.4 Experimental Procedures

3.4.1 Creation of the pM13g plasmid

The construct M13cp was kindly provided by Dr. Andrew Bradbury (CHASTEEN ET AL., 2006). This construct maintains the M13 coding genome as a plasmid with a p15a origin of replication and a chloramphenicol resistance selectable marker. In order to use this construct in *E.coli* XL2-Blue MRF', which is already resistant to chloramphenicol, the chloramphenicol cassette was replaced with a gentamicin resistance gene amplified from the pFastBac1 plasmid. The gentamicin cassette was amplified using primers prJLP001 (5' GGCGACGCGTGCAAATTGCCCGTCGTATTA) & prJLP003 (5' GGCGACGCGTGGAGTATACGTAGCCAACCA), which each contain a MluI restriction endonuclease recognition site near their 5' end. The product of the PCR was cleaned up using a Qiagen PCR clean-up kit and digested with MluI. This product was ligated into M13cp in which the chloramphenicol cassette had been digested out with MluI and gel purified away. The ligation was transformed into *E.coli* and the resulting clones check by

restriction digest. Clones were functionally tested by transformation into *E.coli* XL2-Blue MRF'/ pDHJS AN+ and assaying for phagemid expression. A successful clone was transformed into DH5α and made chemically competent.

3.4.2 Insertion of the attB/attP sites

Oligonucleotides containing the attB and attP sites plus appropriate sticky ends were obtained (IDT) and annealed using a thermocycler. For the attB site, the plasmids were cut with BglII and EcoRI, and the annealed oligonucleotides were ligated. In the resulting plasmid, the BglII site no longer exists. Because of methylation of the XbaI site at the 5' end of the second loxP site, additional nucleotides were added and the SphI (for "S" plasmids) or NheI (for "N" plasmids) set of oligonucleotides were used. Plasmids containing the attB site were digested with NdeI and either NheI or SphI, and the annealed oligonucleotides were ligated in. The NdeI site was mutated in the final plasmid.

Table 6: Primers for inserting attB and attP into the pDHJS plasmids.

Name	Sequence
attB F	GATCGCGCGGTGCGGGTGCCAGGGCGTGCCCTTGGGCTCCCCGGGCGCGTACTG
attB R	AATTCAGTACGCGCCCGGGGAGCCCAAGGGCACGCCCTGGCACCCGCACCGCGA
attP F (SphI)	CGCACACAATTGATGACTTGATCTAGAGTAGTGCCCCAACTGGGGTAACCTTTGAGTTCTCTC AGTTGGGGGCGTAGG
attP R (SphI)	ATATCCTACGCCCCCAACTGAGAGAACTCAAAGGTTACCCCAGTTGGGGCACTAC TCTAGA TCAAGTCATCAATTGTGTGCGCATG
attP F (NheI)	CTAGCGCACACAATTGATGACTTGATCTAGAGTAGTGCCCCAACTGGGGTAACCTTTGAGTTC TCTCAGTTGGGGGCGTAGG
attP R (NheI)	ATATCCTACGCCCCCAACTGAGAGAACTCAAAGGTTACCCCAGTTGGGGCACTACTCTAGAT CAAGTCATCAATTGTGTGCC

3.4.3 Purification of ϕC31 integrase

The construct pHS62, containing the full coding sequence of ϕC31 integrase, was kindly provided by Margaret Smith (THORPE & SMITH, 1998). A ten residue Histidine tag was added to the N-terminus of the integrase by cloning a small, double-stranded DNA fragment created from complimentary oligonucleotides into a NdeI site at the 5' end of the gene using standard methods. The orientation of the insert was confirmed by restriction digestion. The resulting plasmid was named pHPhiC31Int. This plasmid was transformed into BL21 cells using standard procedure.

An overnight culture of BL21 cells containing the plasmid were diluted to OD_{600} = 0.1. Cells were grown at 25°C until OD_{600} = 0.6, then grown at 18°C until OD_{600} = 0.8. Cells were then induced with 0.1 mM IPTG and grown overnight. Cells were pelleted and frozen. Cell pellet was resuspended in Lysis Buffer (150 mM Hepes pH 7.0, 100 mM NaCl, 10% glycerol) with 1 mg/mL lysozyme and incubated on ice for 1 hour. Cell lysate was then sonicated. One volume of 2 M NaCl was slowly added, followed by one volume of 1 M NaCl, 18% PEG 8k. Solution was slowly stirred for 30 min, followed by centrifugation at 20,000x*g* for 20 min. The supernatant was applied to a nickel metal affinity column (Qiagen), which was subsequently washed with ten column volumes each of Wash I (50 mM Hepes pH 7.0, 1 M NaCl, 10% glycerol) and Wash II (50 mM Hepes pH 7.0, 100mM NaCl, 10% glycerol, 50 mM imidazole). Protein was eluted in 1 mL fractions with Elution buffer (50 mM Hepes pH 7.0, 500mM NaCl, 10% glycerol, 400

mM imidazole). Bradford reagent (BioRad) was used to find the peak fractions, which were then pooled and dialyzed into Storage Buffer (50 mM Hepes pH 7.0, 500 mM NaCl, 50% glycerol). All buffers were at 4°C and contained 2.5 mM 2-mercaptoethanol and 0.1 mM PMSF.

3.4.3 Creation of the quadruple HJ substrate

The quadruple HJ substrate was constructed like the dHJ substrate (PLANK & HSIEH, 2006), with the exceptions outlined in this paper. Briefly, single colonies of DH5α cells containing both pM13g and one of the pDHJS-ϕC31 plasmids were grown in Terrific Broth (with chloramphenicol and gentamicin) until bacteria were visible, then inoculated into a large culture and grown overnight. Phage was precipitated from the cell media. Phage were lysed, and the ssDNA circles were purified over a DEAE column (Qiagen). The ssDNA circles were appropriately combined using Reverse Gyrase, linearized with XhoI, and recombined with 5 ng/μL ϕC31 Integrase at 30°C. (Integrase buffer: 10 mM Tris pH 7.0, 1 mM EDTA, 100 mM NaCl, 5% glycerol, 5 mM spermidine, 5 mM DTT, 0.5 mg/mL BSA.) Reaction products were purified over a DEAE column (Qiagen), and run on an agarose gel to separate the large and small heterodimers. The small heterodimers were purified from the gel and combined using Reverse Gyrase. The final product was purified using phenol/chloroform extraction and ethanol precipitation.

3.4.5 Quadruple HJ substrate dissolution

Dissolution of the quadruple HJ substrate was performed as in (CHEN ET AL., 2012).

3.4.6 Creation of the DHJS-2

DHJS-2 was produced as in (WEBB ET AL., 2007) with the exceptions in this paper. Specifically, the starting plasmids contained the attB/attP sites, and the ssDNA was produced using the pM13g system.

3.4.7 Migration of the DHJS-2

The UvsW migration of DHJS-2 was performed as in (WEBB ET AL., 2007).

3.4.8 Electron microscopy

DNA samples (~100 ng) were incubated with gp32 or no protein as appropriate. The protein-DNA complexes were fixed with 0.6% glutaraldehyde (v/v) for 10 min at room temperature followed by gel filtration using a 1 mL Bio-Gel A-5m (BioRad) column to remove free protein and fixatives.

The samples were prepared for electron microscopy as described previously (GRIFFITH & CHRISTIANSEN, 1978). Briefly, the samples were adsorbed to thin carbon foils supported by 400-mesh copper grids in the presence of spermidine, then washed with a water/ethanol series, air dried, and rotary shadowcast with tungsten. The grids were visualized in a Tecnai. Images for publication were captured with the Digital Micrograph software.

4. Insights into the mechanism of double Holliday junction dissolution

4.1 Introduction

Homologous recombination is an important process for faithful DNA repair in the cell. Bloom's helicase (Blm) plays many important roles in ensuring legitimate recombination, as hyperrecombination, loss of heterozygosity, and rearranged gene chromosome architecture are evident in its absence (CHAGANTI ET AL., 1974; KILLEN ET AL., 2009; LAROCQUE ET AL., 2011). On the molecular level, Blm works with Topoisomerase IIIα (Top3α) to convergently migrate double Holliday junctions (dHJ's) (PLANK ET AL., 2006), an intermediate of homologous recombination (BZYMEK ET AL., 2010).

Although there is some evidence that free Blm protein forms hexamers through its N-terminus (BERESTEN ET AL., 1999; KAROW ET AL., 1999), the exact complex on DNA is not known. The RuvB component of the *E. coli* HJ resolving complex, RuvABC, forms hexamers on either side of the HJ, which it then migrates (MAYANAGI ET AL., 2008). Recent biochemical work, however, suggests that the optimal number of Blm molecules per junction is only three to four (MAZINA ET AL., 2012). In addition, several studies show that Blm is required for Top3α to localize to DNA (JOHNSON ET AL., 2000; WU ET AL., 2000; HU ET AL., 2001), suggesting that Blm binds first and recruits Top3α.

It has been suggested that Blm has the ability to convergently migrate the double HJ's to the hemicatenane stage (where one linkage between single strands remains), at which point Top3α is required to undo the hemicatenane (CHEOK ET AL., 2005; WEINSTEIN & ROTHSTEIN, 2008). Using noncognate topoisomerases, Cejka *et al.* were able to trap a migration intermediate, in which the junctions are closer but are not resolved (CEJKA ET AL., 2010). Although it is possible that this structure is a hemicatenane, it is unclear from their data.

In this study, we address the complex formation and activity of Blm and Top3α on Holliday junctions. Both enzymes localize to HJ's, act together processively, and are required for extensive branch migration. Direct visualization of the proteins on DNA and of the migration intermediate structure provide valuable information on the formation and mechanism of the complex.

4.2 Results

4.2.1 Localization to Holliday junctions

Although the affinity of Blm for HJ's has been well documented (KAROW ET AL., 2000; HUBER ET AL., 2006), the exact complex formed is unknown. In addition, the preference of Top3α is less well defined. While Top3α requires a region of ssDNA to perform its enzymatic function, the enzyme also binds to dsDNA through its C terminus (CHEN ET AL., 2012). We further investigated the binding preferences of Blm and Top3α

using EMSA (electrophoretic mobility shift assay), DNase I footprinting, and electron microscopy.

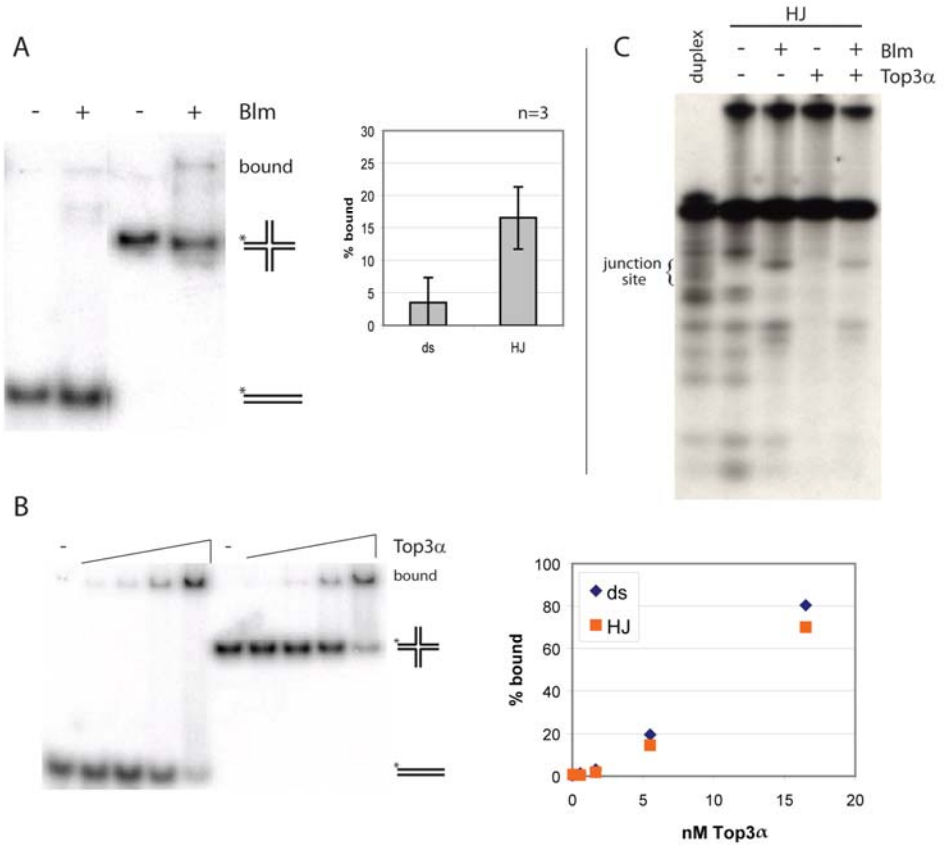

Figure 18: EMSA and DNase I footprinting of Blm and Top3α on duplex vs. HJ.
A. EMSA of Blm binding to duplex and HJ DNA structures, with quantification on the right. HJ's are clearly preferred. **B**. EMSA of Top3α gradient binding to duplex and HJ structures. Top3α does not display a preference. **C**. DNase I footprinting of Blm and Top3α on the HJ structure. While Blm shifts the junction site, Top3α provides protection along its length.

Previous studies have shown that Blm is required for localization of Top3α to discrete foci on chromatin (JOHNSON ET AL., 2000; WU ET AL., 2000; HU ET AL., 2001). Using EMSA on oligonucleotide-based duplex and HJ-mimic structures, we found that

Blm does exert a preference for the junction, while Top3α does not (Figure 18A & B). In addition, Blm causes a deformation of the junction in an HJ substrate, while Top3α provides protection along its entire length (Figure 18C).

Blm and Top3α were each directly visualized on dHJ substrates by being crosslinked to the DNA and then spread for electron microscopy. Blm displayed a strong preference for junctions, binding at the junction, rather than on a duplex arm, in 85% of bound molecules (Table 7). Surprisingly, Top3α also displayed a preference for junctions, localizing to them on 70% of bound molecules. At the concentrations used, DNA molecules rarely contained more than one site of protein binding. Out of 86 molecules observed, only 2 showed Blm binding separately at both junctions. Top3α binding at more than one site was not observed.

Table 7: Counts of Blm and Top3α binding to dHJ substrate by electron microscopy.

Blm	count	%
at one junction	61	62.2
at both junctions	2	2.0
away from junction	13	13.3
connecting two molecules	22	22.4

Top3a	count	%
at one junction	59	71.1
away from junction	24	28.9

4.2.2 Blm forms a higher order complex on HJ's

To determine the number of Blm molecules bound at the junctions, we measured the radius of the observed protein, converted the radius to molecular weight (assuming a globular protein), and compared this to a Blm monomer. Blm at the junctions was

consistent with a mix of monomer and dimer structures, although it is difficult to distinguish between the two at this resolution. Interestingly, in ~25% of bound molecules, Blm was in a large complex that brought together two dHJ substrate molecules (Figure 19). In these complexes, Blm corresponded to a tetramer or larger, indicating that Blm may bind junctions as a dimer, then tetramerize to bring together junction sites.

Bound Top3α corresponded to a monomer or dimer complex. Due to extensive aggregation, higher order complexes involving Top3α were not analyzed.

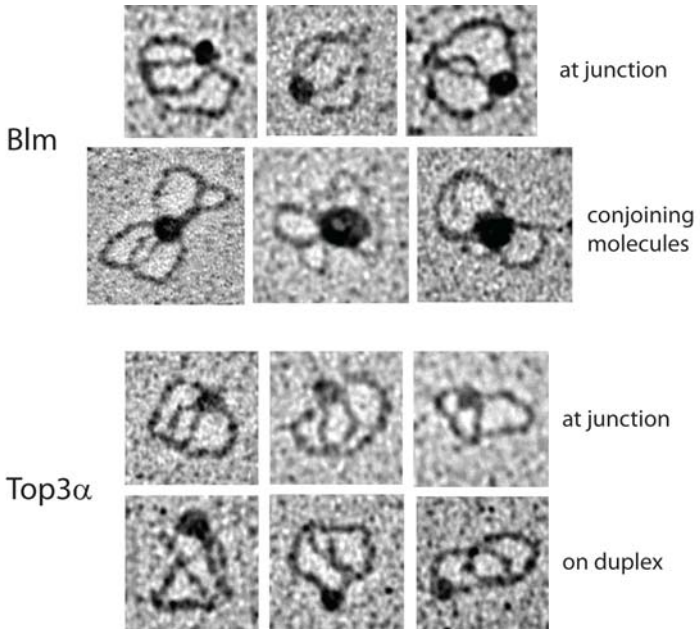

Figure 19: Electron microscopic images of Blm and Top3α binding to dHJ substrate. Electron microscopic images of Blm and Top3α individually binding to dHJ substrate. Blm is seen both at individual junctions and spanning the junctions of multiple molecules. Top3α binds both at junctions and at distal sites on the substrate.

4.2.3 A non-specific topoisomerase creates an intermediate structure

It has previously been shown that using a noncognate topoisomerase creates a "convergently branch migrated" (CBM) intermediate (CEJKA ET AL., 2010). The CBM runs slower on the gel than the starting substrate due to the expansion of the loop regions outside of the junctions (the blue and red loops), as the junctions move closer to each other. Using *Drosophila* Top1, a type IB topoisomerase, we were able to create a similar CBM structure (Figure 20).

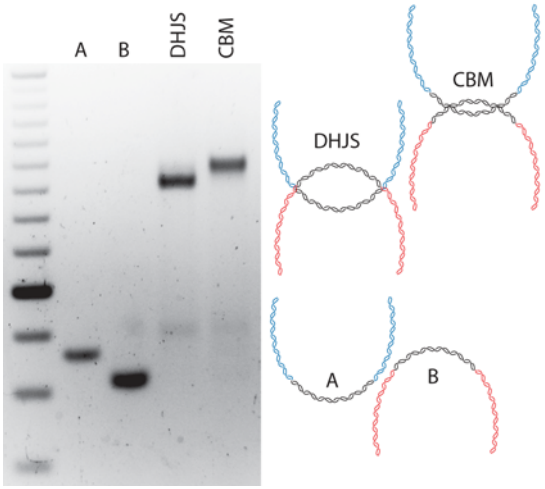

Figure 20: A non-specific topoisomerase creates a CBM intermediate.
Using the non-specific topoisomerase Top1 (a type IB), a "convergently branch migrated" (CBM) intermediate can be created. Substrate was digested with BamHI after the enzymatic reaction, before being run on the agarose gel.

4.2.4 dHJ dissolution is processive

Using the CBM as an intermediate control, we looked at a time course of the dissolution reaction with Blm and Top3α. The time course of dHJ dissolution reveals no intermediate accumulation prior to product formation, indicating that the dissolution

reaction is extremely processive (Figure 21). While product begins to appear at five minutes, at no point was there accumulation of a band corresponding to the CBM.

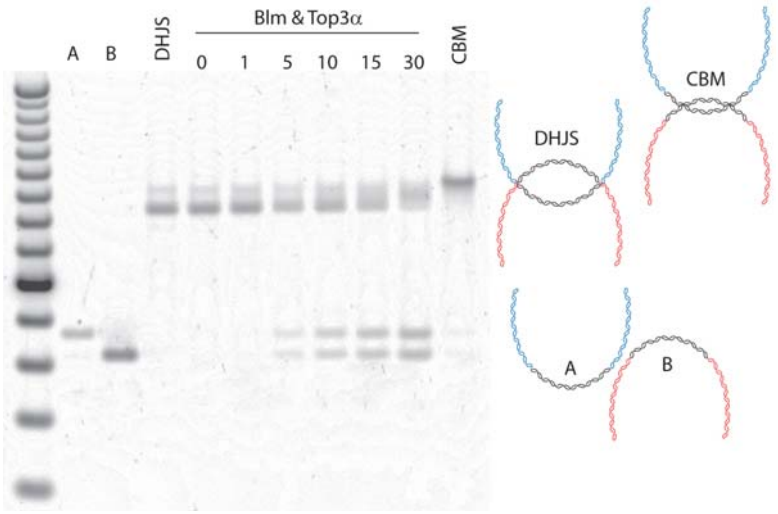

Figure 21: Time course of the dissolution reaction.

Time course of the dissolution reaction using Blm and Top3α, with the CBM intermediate as a control. Product begins to form, around 5 minutes, prior to accumulation of a CBM-sized molecule. Time is in minutes. Substrate was digested with BamHI after the enzymatic reaction, before being run on the agarose gel.

4.2.5 The CBM intermediate is not a hemicatenane

Previously, several groups have suggested that Top3α is only needed for resolving the final hemicatenane in the reaction, suggesting that the CBM may be a hemicatenane. To test this idea, we attempted to resolve the substrate with Top3α alone. Dissolution did not occur with Top3α alone, indicating that the CBM is unlikely to be a hemicatenane (Figure 22). Blm and Top3α together were able to dissolve the substrate, suggesting that the CBM still retains some dHJ-like structure.

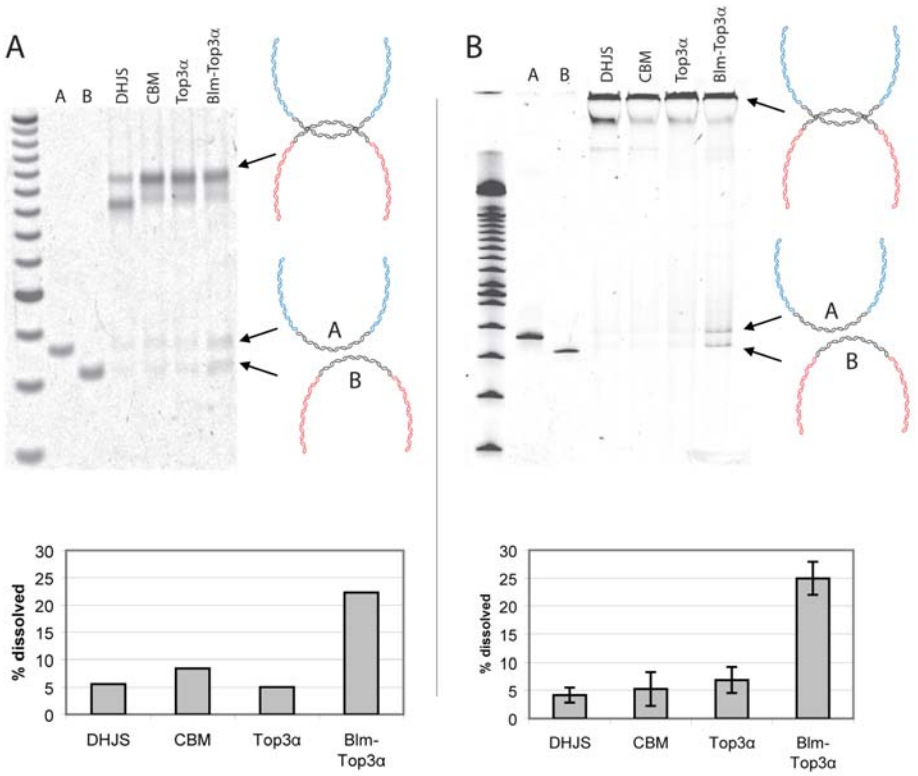

Figure 22: Dissolution of the CBM intermediate requires both Blm and Top3α.

A. CBM intermediate with just Top3α or Blm & Top3α, on an agarose gel, quantified below. **B**. CBM intermediate with just Top3α or Blm & Top3α, on an acrylamide gel, quantified below. Although acrylamide gives a lower background, the difference between DHJS and CBM is unclear, so the agarose gel was run as a control. Substrates were digested with BamHI after the enzymatic reaction, before being run on the agarose or acrylamide gel.

To directly visualize the structure of the CBM, we employed electron microscopy. After the CBM reaction, proteins were digested away with proteinase K, and the protein-free DNA was mounted on the grid. The structures were divided into several categories according to shape (Figure 23A). "Unreacted" structures are those that resemble dHJ substrate alone, prior to reaction (as in Figure 12). "Bar" structures have a squashed, bar-like structure between the two junctions, rather than two loops with space

in between. “Loop” substrates retain space between the two loops in the interjunction area, but this region is significantly smaller than in unreacted molecules. “Circle” molecules are the individual circles resulting from successful dissolution. Shape determination was made by eye.

The length of the large loops outside of the junctions of each shape were measured, and these corresponded well to the predicted distances (Figure 23B). To determine the distance between the junctions, the outer loop measurements were subtracted from the total length of the molecule. While the majority of the junctions were closer together than unreacted substrate, they remained around 80 bp apart from each other, on average. The smallest distance measured corresponded to approximately 20 bp, well shy of a hemicatenane. The shape of the interjunction region (“bar” vs. “loop”) had no effect on the interjunction distance obtained. These results indicate that Top1 is not sufficient to allow Blm to perform complete branch migration.

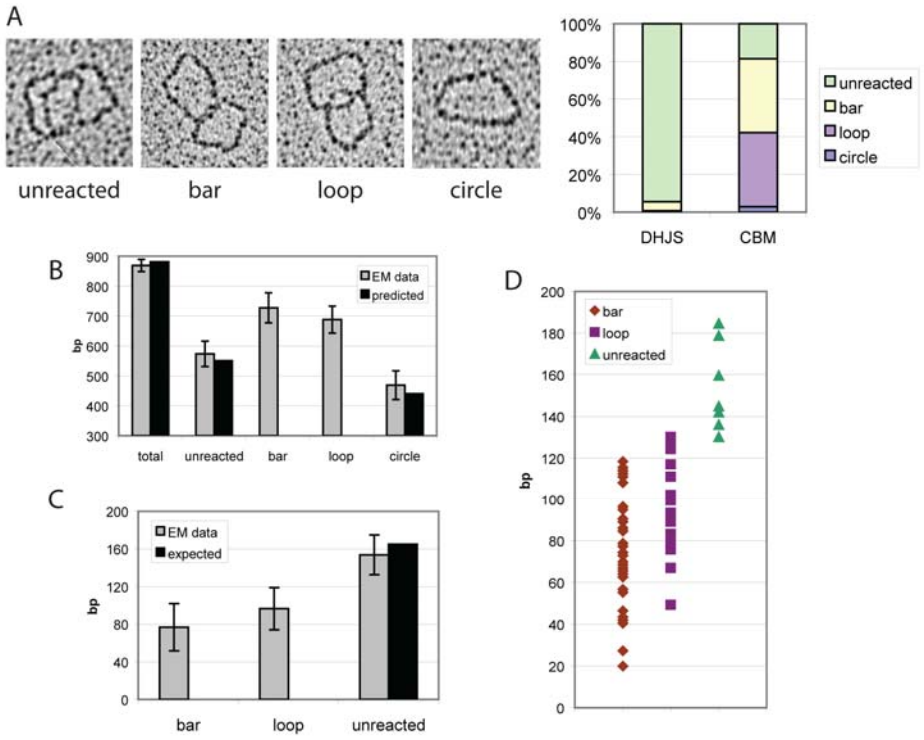

Figure 23: Electron microscope measurements of the interjunction distance in CBM intermediates.

A. Examples of the classes of molecules observed by electron microscopy. The percentages of each type in starting (DHJS) and final (CBM) substrate are shown on the right. **B**. Measurements of the length of the molecules excluding the region between the junctions. "Total" is the complete length of the molecule, measured on unreacted molecules. Measurements were taken in nm and converted to bp. **C**. Length of the distance between the junctions, measured by difference (total theoretical length minus measured distance excluding the junctions). **D**. Graph of data points of distance between junctions.

4.3 Discussion

Although Blm and Top3α are known to dissolve double Holliday junction structures, many details of the mechanism remain unknown. Gel filtration suggests a 1:1 complex of the helicase and topoisomerase (along with the Rmi proteins, which are not present in *Drosophila*)(XU ET AL., 2008), but the exact functional stoichiometry and

conformation of the complex have not been determined. The arrangement of the complex at the junction is also a mystery, although it is suggested that Blm binds first and recruits Top3α. In addition, an early model proposed that the topoisomerase is only needed to undo a hemicatenane that could be created from the dHJ by Blm. By direct observation, we have been able to contribute towards these propositions.

Prior work has characterized the affinity of Blm for HJ's, which appears to be contributed by the HRDC domain (KIM & CHOI, 2010). Using EMSA, DNase I footprinting, and electron microscopy, we confirmed that Blm prefers to bind at the junction site.

We also observed that Blm can form higher order structures at the junctions. Blm at the junction was in the monomer/dimer range, while complexes involving multiple dHJ substrates involved a Blm tetramer or higher complex, indicating that Blm dimers may interact to bring junctions together. The ability to bring together HJ's may be important for Blm in sensing the proper directionality required for dissolution to occur, or may simply be bringing together regions of the DNA that require attention. Although previous studies have observed Blm forming a hexamer in the absence of DNA (KAROW ET AL., 1999) and isolated N-termini of Blm can also form hexamers (BERESTEN ET AL., 1999), we did not observe hexameric complexes on either side of single junctions, as are observed with RuvB (MAYANAGI ET AL., 2008). As RuvB is loaded by the RuvA tetramer,

the RuvAB complex likely represents a completely different class of branch migration activity.

In most cases, Blm bound to only one junction, and was rarely seen to bind separately at both junctions; this may be a function of the concentrations of protein and crosslinking agent used in this study, or because Blm on proximal junctions tends to form a higher order complex. Most of the large Blm complexes appeared to involve two separate dHJ molecules, although the size of the tetramer somewhat obscures the DNA structure. This may indicate that Blm prefers to bring together distal junctions.

Surprisingly, direct observation of Top3α revealed that it also exhibited a preference for binding at the junctions, despite not exhibiting a preference in EMSA studies. This may be due to the differing properties of non-mobile oligonucleotide-based HJ's versus larger, topologically constrained junctions. The constrained junctions likely exhibit different characteristics than a free, nonmobile junction, such as more exposed bases at the junction due to the obligate bending of the DNA arms involved. It is also possible that Top3α's interaction with the junction is more transient, and was therefore captured with crosslinking but was not stable throughout the EMSA procedure. While several groups have shown that Blm is needed for Top3α localization to chromatin, the exact structure of that chromatin was not investigated, and may be a more complex structure.

Originally, several groups proposed that Blm performed the branch migration alone, and Top3α was only needed to undo the final hemicatenane (CHEOK ET AL., 2005; WEINSTEIN & ROTHSTEIN, 2008). On a substrate mimicking the last few links between dHJ's, non-interacting Blm and Top3α were able to undo the substrate (WU ET AL., 2005). However, long distance branch migration of topologically constrained DNA will necessarily create supercoiling stress that must be relieved by a topoisomerase. Using a version of the dHJ substrate containing a mismatch ~40 bp away from the junction, Plank *et al.* were unable to detect migration with Blm alone (PLANK ET AL., 2006).

In this study, we employ a type IB topoisomerase, which will bind to and relax double-stranded DNA, to eliminate the supercoiling stress resulting from branch migration. To allow convergent branch migration, supercoiling stress must be relieved in the region between the two junctions. As this distance decreases, the availability of DNA duplex for the topoisomerase is limited. Surprisingly, despite the presence of one strong band on the gel, electron microscopy revealed a variety of different DNA species with different interjunction distances.

Two distinct species, apart from unreacted and product, were observed in the CBM intermediate samples. These were dubbed "bar" and "loop" based on the structure of the inter-junction DNA. We originally thought that the "bar" phenotype may be an obligate result of the Blm and Top1 migration, as the junctions approach and the DNA distorts in shape; however, some "bar" molecules are present in unreacted samples, and

there is no real difference between the distance of branch migration achieved in "bar" or "loop" substrate structures. However, the "bar" structure may be a form of DNA described as "paranemic crossover" (WANG ET AL., 2010), in which homologous strands are able to interact and form a unique tertiary structure. Although the authors found this structure to be supercoiling-dependent, there may be some residual supercoiling in our original substrate, and supercoiling certainly increases during branch migration. The "bar" and "loop" structures achieve similar inter-junction distances, and it is clear that branch migration stops well before the hemicatenane stage.

A time course of the Blm-Top3α dissolution reaction reveals that dissolution is extremely processive, as no intermediates are visibly formed. Previously, two models were proposed for the mechanism of dHJ dissolution (PLANK & HSIEH, 2009). In the "HJ Migration" model, the two enzymes act together at the junction to perform migration and strand passage. In the "Unravel & Unlink" model, one complex would act first to melt the intervening region, followed by another to perform strand passage. The lack of intermediates favors the first model, in which both activities occur concomitantly.

Previous studies using a non-interacting Top3α and RPA seem to favor the second model, in that melted regions created by Blm could be held apart by RPA and then unlinked by the truncated (non-interacting) topoisomerase (CHEN ET AL., 2012). In yeast, the Rmi protein, another member of the dissolution complex in many species,

stimulated the decatenation step only, which also suggests a separation of functions (CEJKA ET AL., 2010). More work is needed to distinguish these two models.

4.4 Experimental Procedures

4.4.1 Protein purification

Recombinant *Drosophila* Blm and Top3α were purified as in (CHEN ET AL., 2012). Recombinant *Drosophila* Top1 was purified as in (SHAIU & HSIEH, 1998).

4.4.2 DNA binding (EMSA)

Oligonucleotides were radiolabeled with ATP[γP^{32}] (Perkin Elmer) using T4 polynucleotide kinase (NEB). Oligonucleotides were purchased from IDT (Table 5). Where required, oligonucleotides were annealed at a 1:3 hot:cold ratio by temperature gradient in a thermocycler. Substrates were subsequently run on an 8% TBE polyacrylamide gel, excised, and electroeluted. Labeled DNA (0.25 nM) was incubated with 30 nM of protein in 40 mM Tris pH 7.5, 50 mM NaAc, 4 mM $MgCl_2$, 1 mg/mL BSA, 10 mM DTT for 30 min at 4˚C. Loading buffer was added, and samples were run on an 8% TBE polyacrylamide gel overnight at 4˚C. The gel was exposed to a phosphorimager screen and scanned using a Storm scanner.

4.4.3 DNaseI footprinting

Protein (40 nM Blm and/or Top3α) was incubated with radiolabeled HJ (1.4 nM) for 30 min. Magnesium chloride and calcium chloride were then added to a final concentration of 10 mM and 5 mM, respectively. Dnase I was added to 1 ng/μL and

incubated at room temperature for 1 min. Reaction was stopped with an equal volume of Stop Mix (20 mM EDTA, 200 mM NaCl, 1% SDS). DNA was then recovered by phenol/chloroform extraction and ethanol precipitation. DNA was resuspended in formamide, heated at 95°C for 2 min, and loaded onto an 8% acrylamide containing urea and 1x TTE buffer. Gel was run at 300V for 3 hours and exposed to a phosphorimager screen overnight.

4.4.4 Electron microscopy

DNA samples (~100 ng) were incubated with Blm (30 nM), Top3α (50 nM), excess gp32, or no protein as appropriate. The protein-DNA complexes were fixed with 0.6% glutaraldehyde (v/v) for 10 min at room temperature followed by gel filtration using a 1 mL Bio-Gel A-5m (BioRad) column to remove free protein and fixatives.

The samples were prepared for electron microscopy as described previously (GRIFFITH & CHRISTIANSEN, 1978). Briefly, the samples were adsorbed to thin carbon foils supported by 400-mesh copper grids in the presence of spermidine, then washed with a water/ethanol series, air dried, and rotary shadowcast with tungsten. The grids were visualized in a Tecnai. Images for publication were captured with the Digital Micrograph software.

4.4.5 dHJ substrate dissolution/time course

Dissolution reactions were performed as in (CHEN ET AL., 2012). For the time course, reactions were stopped after the appropriate incubation time by the addition of

SDS and EDTA, then processed as above. Reactions were run on a 1.9% TAE agarose gel containing 0.5 μg/mL ethidium bromide at 4V/cm for 6-8 hours, which was destained prior to imaging.

4.4.6 Creating the CBM intermediate

Conditions for creating the CBM intermediate were identical to dHJ dissolution, except that 300 nM *Drosophila* Top1 was added in place of Top3α.

5. Summary and Perspective

5.1 Summary

Prior work in the lab demonstrated that Top3α and Blm are uniquely able to convergently migrate dHJ's into solely non-crossover products. This work sought to further elucidate this process, including why the reaction is specific to Top3α, creating a better way to produce HJ substrates, and observing reaction intermediates.

Because Top3α differs from its isozyme (Top3β) in its C-terminal region, we characterized the unique C-terminus of Top3α. The Top3α CT is required for viability in *Drosophila*, and contributes the functions of binding to Blm and binding duplex DNA. In addition, the *Drosophila* Top3α CT contains an insert region (CT2) which can independently bind Blm and may provide some of the functions of the missing Rmi proteins. Absence of this region in *Drosophila* led to a sharp decrease in viability, indicating an important *in vivo* role.

The dHJ substrate used in these studies is quite time consuming to create. In order to streamline the process, we have introduced the pM13g system of constitutive phagemid expression. The production of ssDNA is the rate limiting step for creating any of the HJ substrates, and use of this plasmid makes the process considerably easier. We also swapped the Cre/lox recombination system for the ϕC31 integrase unidirectional recombination system, which creates a quadruple HJ substrate; we have shown that the quadruple HJ substrate functions exactly like the dHJ substrate in enzymatic reactions.

We addressed the hypotheses that Blm is required to localize Top3α to junctions and that Blm alone is sufficient to migrate the dHJ's into a hemicatenane structure. While EMSA's showed that Top3α had no preference for junctions (while Blm, as expected, showed a strong preference), crosslinking and electron microscopy showed that Top3α bound to junctions over duplex at an almost 3:1 ratio, suggesting that Top3α may localize to such sites, at least transiently, on its own. The Blm-Top3α dissolution reaction is very processive, and an intermediate can only be seen when a non-specific topoisomerase (Top1) is used. However, despite the presence of this duplex-relaxing enzyme, the junctions remain ten's of base pairs apart. Top3α is therefore an essential component for migration as well as decatenation.

5.2 Future Directions

5.2.1 "BTR" complex formation

The dHJ dissolution complex (referred to in the literature as "BTR" for Blm-Top3α-Rmi) still has many mysteries to be unraveled. Although many recent studies, including this one, have helped to parse out the role of each component, the way in which the entire complex functions as a whole remains to be elucidated.

Although there is evidence that the complex exists in a 1:1:1:1 ratio (Blm:Top3α:Rmi1:Rmi2) (XU ET AL., 2008), the exact stoichiometry of the complex remains to be definitively determined. Early work suggested that Blm forms hexamers (BERESTEN ET AL., 1999; KAROW ET AL., 1999), in the manner of RuvB. However, recent

biochemical work suggests that the optimal stoichiometry for migrating junctions is three to four monomers per junction (MAZINA ET AL., 2012). Blm also contains two putative Top3*α* binding domains (WU ET AL., 2000), suggesting a 1:2 stoichiometry of Blm:Top3*α*.

Another important component, highlighted in this work, is the DNA upon which the complex acts. Although the complex is known for its unique dHJ dissolution activity, it is proposed that Top3*α* may assist Blm on many of its other substrates, including D-loops and anaphase bridges (BACHRATI ET AL., 2006; CHAN ET AL., 2007). Presumably, the complex forms so that the enzyme active sites have access to all of these substrates. In addition, many of these substrates require a unique directionality of migration for productive dissolution, suggesting that the complex itself may dictate a direction. One recent study showed that Blm does have a slight migration bias on Holliday junctions based on its 3'-5' directionality (MAZINA ET AL., 2012). Future work will be required to determine the way the complex forms on DNA and if complex formation affects its activity.

5.2.2 Mechanism of dHJ dissolution

Recently, two models have been put forth to explain how the helicase and topoisomerase activities are able to achieve dHJ dissolution (PLANK & HSIEH, 2009) (Figure 24). Inherent in each is the understanding that topological strain will increase ahead of junction migration, and that Holliday junctions deform the DNA in a way

which does not normally allow them to be in close proximity to each other. The persistence length of DNA is generally considered to be around 50 nm (MANNING, 2006), meaning that junctions closer than 75 base pairs require deformation of the DNA duplex.

In the "Unwind & Unlink" model, a melting step is proposed, in which the DNA duplexes are first converted to single strands by Blm so that the flexibility of the region between the junctions is increased, allowing the junctions to approach each other. Top3α would then perform strand passage to decatenate the strands. Although stimulation by the single-stranded binding protein RPA (Chapter 2) suggests that this is the case, more definitive evidence is needed.

The "HJ Migration" model proposes that the two enzymes perform their activities concomitantly. The processivity of the complex (Chapter 4) suggests that the activities are concomitant at the junction, as in the HJ Migration model. Further work is needed to more clearly define this mechanism.

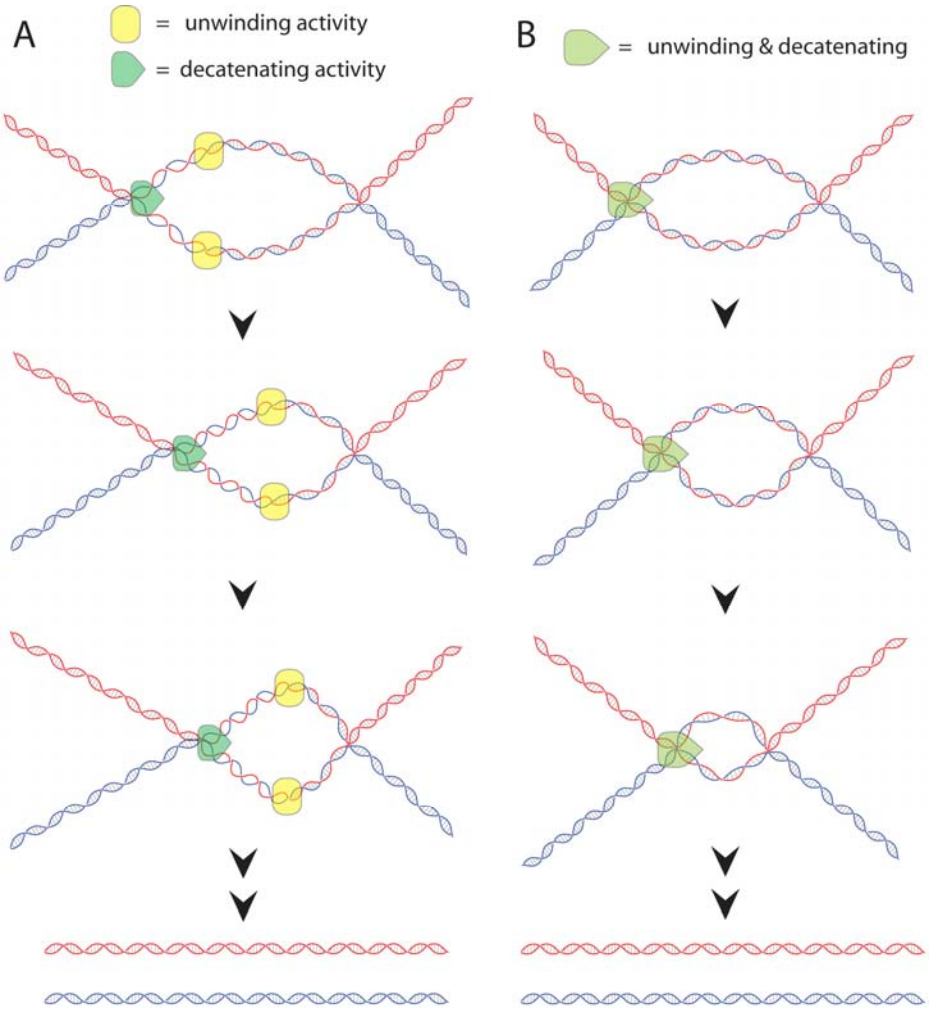

Figure 24: Two models of the mechanism of dHJ dissolution.
A. A diagram of the "Unwind & Unlink" model, in which the helicase first melts the duplex strands (with the topoisomerase to relieve supercoiling stress) followed by the topoisomerase unlinking the strands (with the helicase to help re-anneal the strands). **B**. A diagram of the "HJ Migration" model, in which the helicase and topoisomerase work together to simultaneously migrate the junctions and unlink the strands.

5.2.3 Structure of the C-terminus of Top3α

This work proposes several functions of the Top3α C-terminus that require this region to act as a scaffold, including binding to other proteins and to DNA. There is no

structure of metazoan Top3α, although the tail region is predicted to resemble other zinc finger containing proteins (using the modeling prediction software PHYRE). Dividing the C-terminus into smaller pieces reduced its binding to both Blm and DNA (CT1 & CT3 vs. CT1,3), suggesting that the regions fold together. Structure studies of this region, perhaps using NMR, in the presence and absence of DNA, could provide valuable insight. This data could be combined with point mutations of conserved residues to further reveal which areas are critical for protein-protein and protein-DNA interactions.

In addition, further studies could elucidate the contributions of the zinc fingers in the C-terminus. Previous studies have shown that the C-terminus of *E. coli* Top1, another type IA topoisomerase, has three zinc-finger motifs and coordinates three to four zinc ions (TSE-DINH & BERAN-STEED, 1988). Mutation or modification of the cysteines in the zinc fingers of Top3α CT could also help to distinguish between the DNA-binding and Blm-binding contributions, although it is also possible that such mutations would destabilize the Top3α CT structure.

5.2.4 Characterization of *Drosophila* mutants

In this work, two new *Drosophila* transgenes were introduced: Top3αNT-YFP and Top3αΔCT2-YFP (Chapter 2). Although the Top3αNT-YFP transgene could not rescue viability, characterization of the method of their demise could still be insightful. It would be interesting to see if the Top3αNT-YFP flies die at the same stage of development as top3α nulls (top3α ^{54}) or hypomorphs (top3α ^{191}) (PLANK ET AL., 2005;

WU ET AL., 2010). The critical stage for the 90-95% of Top3αΔCT2-YFP flies that did not live to adulthood could be compared as well. In addition, the Top3αΔCT2-YFP rescue flies can be further characterized for any defects, such as fertility and lifespan. Although initial results indicate that both sexes of Top3αΔCT2-YFP flies can produce adult offspring when mated to wildtype flies, there may be a reduced ability to do so, as seen in the lower number of progeny from flies with one copy of the transgene. This effect should be further investigated.

5.3 Concluding Remarks

This work has advanced our understanding of the dHJ dissolution complex and opened up new pathways for exploration. While previous work has focused on the helicase, this work highlights the importance of the topoisomerase in the complex. Not only is Top3α an essential enzyme, but the previously uncharacterized C-terminal domain is also an essential component, providing an interaction interface for proteins and DNA. Emerging evidence in the field suggests that Top3α assists Blm in many of its roles, including suppression of somatic recombination, initiation and resolution of double-strand break repair, chromosome segregation, and repair of interstrand crosslinks. Our work on the unique biochemical reaction that these two enzymes perform together can provide insight into how they function in multiple pathways and ultimately promote genome stability.

References

ANDERSEN, S. L., KUO, H. K., SAVUKOSKI, D., BRODSKY, M. H., AND SEKELSKY, J. (2011) Three structure-selective endonucleases are essential in the absence of BLM helicase in Drosophila. *PLoS Genet* **7**, e1002315

BACHRATI, C. Z., BORTS, R. H., AND HICKSON, I. D. (2006) Mobile D-loops are a preferred substrate for the Bloom's syndrome helicase. *Nucleic Acids Res* **34**, 2269-2279

BAREFIELD, C., AND KARLSEDER, J. (2012) The BLM helicase contributes to telomere maintenance through processing of late-replicating intermediate structures. *Nucleic Acids Res*

BAYART, E., DUTERTRE, S., JAULIN, C., GUO, R. B., XI, X. G., AND AMOR-GUERET, M. (2006) The Bloom syndrome helicase is a substrate of the mitotic Cdc2 kinase. *Cell Cycle* **5**, 1681-1686

BEAMISH, H., KEDAR, P., KANEKO, H., CHEN, P., FUKAO, T., PENG, C., BERESTEN, S., GUEVEN, N., PURDIE, D., LEES-MILLER, S., ELLIS, N., KONDO, N., AND LAVIN, M. F. (2002) Functional link between BLM defective in Bloom's syndrome and the ataxia-telangiectasia-mutated protein, ATM. *J Biol Chem* **277**, 30515-30523

BENNETT, R. J., NOIROT-GROS, M.-F., AND WANG, J. C. (2000) Interaction between Yeast Sgs1 Helicase and DNA Topoisomerase III. *J. Biol. Chem.* **275**, 26898-26905

BERESTEN, S. F., STAN, R., VAN BRABANT, A. J., YE, T., NAURECKIENE, S., AND ELLIS, N. A. (1999) Purification of overexpressed hexahistidine-tagged BLM N431 as oligomeric complexes. *Protein Expr Purif* **17**, 239-248

BLANTON, H. L., RADFORD, S. J., MCMAHAN, S., KEARNEY, H. M., IBRAHIM, J. G., AND SEKELSKY, J. (2005) REC, Drosophila MCM8, drives formation of meiotic crossovers. *PLoS Genet* **1**, e40

BROBERG, K., HOGLUND, M., GUSTAFSSON, C., BJORK, J., INGVAR, C., ALBIN, M., AND OLSSON, H. (2007) Genetic variant of the human homologous recombination-associated gene RMI1 (S455N) impacts the risk of AML/MDS and malignant melanoma. *Cancer Letters* **258**, 38-44

BROSH, R. M., JR., KAROW, J. K., WHITE, E. J., SHAW, N. D., HICKSON, I. D., AND BOHR, V. A. (2000) Potent inhibition of werner and bloom helicases by DNA minor groove binding drugs. *Nucleic Acids Res* **28**, 2420-2430

BROSH, R. M., JR., LI, J. L., KENNY, M. K., KAROW, J. K., COOPER, M. P., KUREEKATTIL, R. P., HICKSON, I. D., AND BOHR, V. A. (2000) Replication protein A physically interacts with the Bloom's syndrome protein and stimulates its helicase activity. *J Biol Chem* **275**, 23500-23508

BROWN, T. A., CECCONI, C., TKACHUK, A.N., BUSTAMANTE, C., AND CLAYTON, D.A. (2005) Replication of mitochondrial DNA occurs by strand displacement with alternative light-strand origins, not via strand-coupled mechanism. *Genes & Development* **19**, 2466-2476

BUGREEV, D. V., MAZINA, O. M., AND MAZIN, A. V. (2009) Bloom syndrome helicase stimulates RAD51 DNA strand exchange activity through a novel mechanism. *J Biol Chem* **284**, 26349-26359

BUGREEV, D. V., YU, X., EGELMAN, E. H., AND MAZIN, A. V. (2007) Novel pro- and anti-recombination activities of the Bloom's syndrome helicase. *Genes Dev* **21**, 3085-3094

BUSSEN, W., RAYNARD, S., BUSYGINA, V., SINGH, A. K., AND SUNG, P. (2007) Holliday junction processing activity of the BLM-Topo IIIalpha-BLAP75 complex. *J Biol Chem* **282**, 31484-31492

BZYMEK, M., THAYER, N. H., OH, S. D., KLECKNER, N., AND HUNTER, N. (2010) Double Holliday junctions are intermediates of DNA break repair. *Nature* **464**, 937-941

CAPP, C., WU, J., AND HSIEH, T. S. (2009) Drosophila RecQ4 has a 3'-5' DNA helicase activity that is essential for viability. *J Biol Chem* **284**, 30845-30852

CEJKA, P., PLANK, J. L., BACHRATI, C. Z., HICKSON, I. D., AND KOWALCZYKOWSKI, S. C. (2010) Rmi1 stimulates decatenation of double Holliday junctions during dissolution by Sgs1-Top3. *Nat Struct Mol Biol* **17**, 1377-1382

CHAGANTI, R. S., SCHONBERG, S., AND GERMAN, J. (1974) A manyfold increase in sister chromatid exchanges in Bloom's syndrome lymphocytes. *Proc Natl Acad Sci U S A* **71**, 4508-4512

CHAMPOUX, J. J. (2001) DNA topoisomerases: structure, function, and mechanism. *Annu Rev Biochem* **70**, 369-413

CHAN, K. L., NORTH, P. S., AND HICKSON, I. D. (2007) BLM is required for faithful chromosome segregation and its localization defines a class of ultrafine anaphase bridges. *Embo J* **26**, 3397-3409

CHANG, M., BELLAOUI, M., ZHANG, C., DESAI, R., MOROZOV, P., DELGADO-CRUZATA, L., ROTHSTEIN, R., FREYER, G. A., BOONE, C., AND BROWN, G. W. (2005) RMI1/NCE4, a suppressor of genome instability, encodes a member of the RecQ helicase/Topo III complex. *Embo J* **24**, 2024-2033

CHANGELA, A., DIGATE, R. J., AND MONDRAGON, A. (2007) Structural studies of E. coli topoisomerase III-DNA complexes reveal a novel type IA topoisomerase-DNA conformational intermediate. *J Mol Biol* **368**, 105-118

CHASTEEN, L., AYRISS, J., PAVLIK, P., AND BRADBURY, A. R. (2006) Eliminating helper phage from phage display. *Nucleic Acids Res* **34**, e145

CHEN, C. F., AND BRILL, S. J. (2010) An essential DNA strand-exchange activity is conserved in the divergent N-termini of BLM orthologs. *Embo J* **29**, 1713-1725

CHEN, H., YOU, M. J., JIANG, Y., WANG, W., AND LI, L. (2011) RMI1 attenuates tumor development and is essential for early embryonic survival. *Mol Carcinog* **50**, 80-88

CHEN, S. H., WU, C. H., PLANK, J. L., AND HSIEH, T. S. (2012) Essential functions of the C-terminus of Drosophila topoisomerase IIIalpha in double Holliday junction dissolution. *J Biol Chem*

CHEOK, C. F., BACHRATI, C. Z., CHAN, K. L., RALF, C., WU, L., AND HICKSON, I. D. (2005) Roles of the Bloom's syndrome helicase in the maintenance of genome stability. *Biochem Soc Trans* **33**, 1456-1459

CHESTER, N., KUO, F., KOZAK, C., O'HARA, C. D., AND LEDER, P. (1998) Stage-specific apoptosis, developmental delay, and embryonic lethality in mice homozygous for a targeted disruption in the murine Bloom's syndrome gene. *Genes Dev* **12**, 3382-3393

COBB, J. A., AND BJERGBAEK, L. (2006) RecQ helicases: lessons from model organisms. *Nucleic Acids Res* **34**, 4106-4114

DAVIES, S. L., NORTH, P. S., DART, A., LAKIN, N. D., AND HICKSON, I. D. (2004) Phosphorylation of the Bloom's syndrome helicase and its role in recovery from S-phase arrest. *Mol Cell Biol* **24**, 1279-1291

DAVIES, S. L., NORTH, P. S., AND HICKSON, I. D. (2007) Role for BLM in replication-fork restart and suppression of origin firing after replicative stress. *Nat Struct Mol Biol* **14**, 677-679

DEANS, A. J., AND WEST, S. C. (2009) FANCM connects the genome instability disorders Bloom's Syndrome and Fanconi Anemia. *Mol Cell* **36**, 943-953

DUTERTRE, S., ABABOU, M., ONCLERCQ, R., DELIC, J., CHATTON, B., JAULIN, C., AND AMOR-GUERET, M. (2000) Cell cycle regulation of the endogenous wild type Bloom's syndrome DNA helicase. *Oncogene* **19**, 2731-2738

FRICKE, W. M., KALIRAMAN, V., AND BRILL, S. J. (2001) Mapping the DNA Topoisomerase III Binding Domain of the Sgs1 DNA Helicase. *J. Biol. Chem.* **276**, 8848-8855

GANGLOFF, S., MCDONALD, J. P., BENDIXEN, C., ARTHUR, L., AND ROTHSTEIN, R. (1994) The yeast type I topoisomerase Top3 interacts with Sgs1, a DNA helicase homolog: a potential eukaryotic reverse gyrase. *Mol. Cell. Biol.* **14**, 8391-8398

GERMAN, J. (1993) Bloom syndrome: a mendelian prototype of somatic mutational disease. *Medicine (Baltimore)* **72**, 393-406

GOULAOUIC, H., ROULON, T., FLAMAND, O., GRONDARD, L., LAVELLE, F., AND RIOU, J. F. (1999) Purification and characterization of human DNA topoisomerase IIIalpha. *Nucl. Acids Res.* **27**, 2443-2450

GRIERSON, P. M., LILLARD, K., BEHBEHANI, G. K., COMBS, K. A., BHATTACHARYYA, S., ACHARYA, S., AND GRODEN, J. (2011) BLM helicase facilitates RNA polymerase I-mediated ribosomal RNA transcription. *Hum Mol Genet*

GRIFFITH, J. D., AND CHRISTIANSEN, G. (1978) Electron microscope visualization of chromatin and other DNA-protein complexes. *Annu Rev Biophys Bioeng* **7**, 19-35

HANADA, K., UKITA, T., KOHNO, Y., SAITO, K., KATO, J., AND IKEDA, H. (1997) RecQ DNA helicase is a suppressor of illegitimate recombination in Escherichia coli. *Proc Natl Acad Sci U S A* **94**, 3860-3865

HANAI, R., CARON, P. R., AND WANG, J. C. (1996) Human TOP3: a single-copy gene encoding DNA topoisomerase III. *PNAS* **93**, 3653-3657

HARMON, F. G., DIGATE, R. J., AND KOWALCZYKOWSKI, S. C. (1999) RecQ Helicase and Topoisomerase III Comprise a Novel DNA Strand Passage Function: A Conserved Mechanism for Control of DNA Recombination. *Molecular Cell* **3**, 611-620

HEMPHILL, A. W., AKKARI, Y., NEWELL, A. H., SCHULTZ, R. A., GROMPE, M., NORTH, P. S., HICKSON, I. D., JAKOBS, P. M., RENNIE, S., PAUW, D., HEJNA, J., OLSON, S. B., AND MOSES, R. E. (2009) Topo IIIalpha and BLM act within the Fanconi anemia pathway in response to DNA-crosslinking agents. *Cytogenet Genome Res* **125**, 165-175

HIASA, H., DIGATE, R. J., AND MARIANS, K. J. (1994) Decatenating activity of Escherichia coli DNA gyrase and topoisomerases I and III during oriC and pBR322 DNA replication in vitro. *J Biol Chem* **269**, 2093-2099

HU, P., BERESTEN, S., VAN BRABANT, A., YE, T.-Z., PANDOLFI, P.-P., JOHNSON, F. B., GUARENTE, L., AND ELLIS, N. A. (2001) Evidence for BLM and Topoisomerase III{{alpha}} interaction in genomic stability. *Hum. Mol. Genet.* **10**, 1287-1298

HU, P., BERESTEN, S. F., VAN BRABANT, A. J., YE, T. Z., PANDOLFI, P. P., JOHNSON, F. B., GUARENTE, L., AND ELLIS, N. A. (2001) Evidence for BLM and Topoisomerase IIIalpha interaction in genomic stability. *Hum Mol Genet* **10**, 1287-1298

HUBER, M. D., DUQUETTE, M. L., SHIELS, J. C., AND MAIZELS, N. (2006) A conserved G4 DNA binding domain in RecQ family helicases. *J Mol Biol* **358**, 1071-1080

JOHNSON-SCHLITZ, D., AND ENGELS, W. R. (2006) Template disruptions and failure of double Holliday junction dissolution during double-strand break repair in Drosophila BLM mutants. *Proc Natl Acad Sci U S A* **103**, 16840-16845

JOHNSON-SCHLITZ, D. M., AND ENGELS, W. R. (2006) The effect of gap length on double-strand break repair in Drosophila. *Genetics* **173**, 2033-2038

JOHNSON, F. B., LOMBARD, D. B., NEFF, N. F., MASTRANGELO, M.-A., DEWOLF, W., ELLIS, N. A., MARCINIAK, R. A., YIN, Y., JAENISCH, R., AND GUARENTE, L. (2000) Association of the Bloom Syndrome Protein with Topoisomerase III{{alpha}} in Somatic and Meiotic Cells. *Cancer Res* **60**, 1162-1167

KAPPELER, M., KRANZ, E., WOOLCOCK, K., GEORGIEV, O., AND SCHAFFNER, W. (2008) Drosophila bloom helicase maintains genome integrity by inhibiting recombination between divergent DNA sequences. *Nucleic Acids Res* **36**, 6907-6917

KAROW, J. K., CHAKRAVERTY, R. K., AND HICKSON, I. D. (1997) The Bloom's syndrome gene product is a 3'-5' DNA helicase. *J Biol Chem* **272**, 30611-30614

KAROW, J. K., CONSTANTINOU, A., LI, J. L., WEST, S. C., AND HICKSON, I. D. (2000) The Bloom's syndrome gene product promotes branch migration of holliday junctions. *Proc Natl Acad Sci U S A* **97**, 6504-6508

KAROW, J. K., NEWMAN, R. H., FREEMONT, P. S., AND HICKSON, I. D. (1999) Oligomeric ring structure of the Bloom's syndrome helicase. *Curr Biol* **9**, 597-600

KE, Y., HUH, J. W., WARRINGTON, R., LI, B., WU, N., LENG, M., ZHANG, J., BALL, H. L., AND YU, H. (2011) PICH and BLM limit histone association with anaphase centromeric DNA threads and promote their resolution. *Embo J*

KILLEN, M. W., STULTS, D. M., ADACHI, N., HANAKAHI, L., AND PIERCE, A. J. (2009) Loss of Bloom syndrome protein destabilizes human gene cluster architecture. *Hum Mol Genet* **18**, 3417-3428

KIM, Y. M., AND CHOI, B. S. (2010) Structure and function of the regulatory HRDC domain from human Bloom syndrome protein. *Nucleic Acids Res* **38**, 7764-7777

KUSANO, K., JOHNSON-SCHLITZ, D. M., AND ENGELS, W. R. (2001) Sterility of Drosophila with mutations in the Bloom syndrome gene--complementation by Ku70. *Science* **291**, 2600-2602

KWAN, K. Y., GREENWALD, R. J., MOHANTY, S., SHARPE, A. H., SHAW, A. C., AND WANG, J. C. (2007) Development of autoimmunity in mice lacking DNA topoisomerase 3-beta. *PNAS* **104**, 9242-9247

KWAN, K. Y., MOENS, P. B., AND WANG, J. C. (2003) Infertility and aneuploidy in mice lacking a type IA DNA topoisomerase IIIbeta. *PNAS* **100**, 2526-2531

KWAN, K. Y., AND WANG, J. C. (2001) Mice lacking DNA topoisomerase IIIbeta develop to maturity but show a reduced mean lifespan. *Proc Natl Acad Sci U S A* **98**, 5717-5721

KWAN, K. Y., AND WANG, J. C. (2001) Mice lacking DNA topoisomerase IIIbeta develop to maturity but show a reduced mean lifespan. *PNAS* **98**, 5717-5721

LANGLOIS, R. G., BIGBEE, W. L., JENSEN, R. H., AND GERMAN, J. (1989) Evidence for increased in vivo mutation and somatic recombination in Bloom's syndrome. *Proc Natl Acad Sci U S A* **86**, 670-674

LAROCQUE, J. R., AND JASIN, M. (2010) Mechanisms of recombination between diverged sequences in wild-type and BLM-deficient mouse and human cells. *Mol Cell Biol* **30**, 1887-1897

LAROCQUE, J. R., STARK, J. M., OH, J., BOJILOVA, E., YUSA, K., HORIE, K., TAKEDA, J., AND JASIN, M. (2011) Interhomolog recombination and loss of heterozygosity in wild-type and Bloom syndrome helicase (BLM)-deficient mammalian cells. *Proc Natl Acad Sci U S A*

LENG, M., CHAN, D. W., LUO, H., ZHU, C., QIN, J., AND WANG, Y. (2006) MPS1-dependent mitotic BLM phosphorylation is important for chromosome stability. *Proc Natl Acad Sci U S A* **103**, 11485-11490

LI, W., AND WANG, J. C. (1998) Mammalian DNA topoisomerase IIIalpha is essential in early embryogenesis. *Proc Natl Acad Sci U S A* **95**, 1010-1013

LUO, G., SANTORO, I. M., MCDANIEL, L. D., NISHIJIMA, I., MILLS, M., YOUSSOUFIAN, H., VOGEL, H., SCHULTZ, R. A., AND BRADLEY, A. (2000) Cancer predisposition caused by elevated mitotic recombination in Bloom mice. *Nat Genet* **26**, 424-429

MANKOURI, H. W., ASHTON, T. M., AND HICKSON, I. D. (2011) Holliday junction-containing DNA structures persist in cells lacking Sgs1 or Top3 following exposure to DNA damage. *Proc Natl Acad Sci U S A* **108**, 4944-4949

MANNING, G. S. (2006) The persistence length of DNA is reached from the persistence length of its null isomer through an internal electrostatic stretching force. *Biophys J* **91**, 3607-3616

MAYANAGI, K., FUJIWARA, Y., MIYATA, T., AND MORIKAWA, K. (2008) Electron microscopic single particle analysis of a tetrameric RuvA/RuvB/Holliday junction DNA complex. *Biochem Biophys Res Commun* **365**, 273-278

MAZINA, O. M., ROSSI, M. J., DEAKYNE, J. S., HUANG, F., AND MAZIN, A. V. (2012) Polarity and bypass of DNA heterology during branch migration of Holliday junctions by human RAD54, BLM, and RECQ1 proteins. *J Biol Chem* **287**, 11820-11832

MEETEI, A. R., SECHI, S., WALLISCH, M., YANG, D., YOUNG, M. K., JOENJE, H., HOATLIN, M. E., AND WANG, W. (2003) A multiprotein nuclear complex connects Fanconi anemia and Bloom syndrome. *Mol Cell Biol* **23**, 3417-3426

MULLEN, J. R., NALLASETH, F. S., LAN, Y. Q., SLAGLE, C. E., AND BRILL, S. J. (2005) Yeast Rmi1/Nce4 Controls Genome Stability as a Subunit of the Sgs1-Top3 Complex. *Mol. Cell. Biol.* **25**, 4476-4487

MYUNG, K., DATTA, A., CHEN, C., AND KOLODNER, R. D. (2001) SGS1, the Saccharomyces cerevisiae homologue of BLM and WRN, suppresses genome instability and homeologous recombination. *Nat Genet* **27**, 113-116

NIMONKAR, A. V., OZSOY, A. Z., GENSCHEL, J., MODRICH, P., AND KOWALCZYKOWSKI, S. C. (2008) Human exonuclease 1 and BLM helicase interact to resect DNA and initiate DNA repair. *Proc Natl Acad Sci U S A* **105**, 16906-16911

OUYANG, K. J., WOO, L. L., ZHU, J., HUO, D., MATUNIS, M. J., AND ELLIS, N. A. (2009) SUMO modification regulates BLM and RAD51 interaction at damaged replication forks. *PLoS Biol* **7**, e1000252

PLANK, J. L., CHU, S. H., POHLHAUS, J. R., WILSON-SALI, T., AND HSIEH, T. S. (2005) Drosophila melanogaster topoisomerase IIIalpha preferentially relaxes a positively or negatively supercoiled bubble substrate and is essential during development. *J Biol Chem* **280**, 3564-3573

PLANK, J. L., AND HSIEH, T.-S. (2006) A Novel, Topologically Constrained DNA Molecule Containing a Double Holliday Junction: DESIGN, SYNTHESIS, AND INITIAL BIOCHEMICAL CHARACTERIZATION. *J. Biol. Chem.* **281**, 17510-17516

PLANK, J. L., AND HSIEH, T. S. (2009) Helicase-appended Topoisomerases: New Insight into the Mechanism of Directional Strand-transfer. *J Biol Chem* **284**, 30737-30741

PLANK, J. L., WU, J., AND HSIEH, T.-S. (2006) Topoisomerase III{alpha} and Bloom's helicase can resolve a mobile double Holliday junction substrate through convergent branch migration. *PNAS* **103**, 11118-11123

RALF, C., HICKSON, I. D., AND WU, L. (2006) The Bloom's syndrome helicase can promote the regression of a model replication fork. *J Biol Chem* **281**, 22839-22846

RAYNARD, S., BUSSEN, W., AND SUNG, P. (2006) A double Holliday junction dissolvasome comprising BLM, topoisomerase IIIalpha, and BLAP75. *J Biol Chem* **281**, 13861-13864

RUSSELL, B., BHATTACHARYYA, S., KEIRSEY, J., SANDY, A., GRIERSON, P., PERCHINIAK, E., KAVECANSKY, J., ACHARYA, S., AND GRODEN, J. (2011) Chromosome breakage is regulated by the interaction of the BLM helicase and topoisomerase IIalpha. *Cancer Res* **71**, 561-571

SAN FILIPPO, J., SUNG, P., AND KLEIN, H. (2008) Mechanism of eukaryotic homologous recombination. *Annu Rev Biochem* **77**, 229-257

SARKIES, P., AND SALE, J. E. (2011) Propagation of histone marks and epigenetic memory during normal and interrupted DNA replication. *Cell Mol Life Sci*

SEKI, M., NAKAGAWA, T., SEKI, T., KATO, G., TADA, S., TAKAHASHI, Y., YOSHIMURA, A., KOBAYASHI, T., AOKI, A., OTSUKI, M., HABERMANN, F. A., TANABE, H., ISHII, Y., AND ENOMOTO, T. (2006) Bloom helicase and DNA topoisomerase IIIalpha are involved in the dissolution of sister chromatids. *Mol Cell Biol* **26**, 6299-6307

SEKI, T., SEKI, M., ONODERA, R., KATADA, T., AND ENOMOTO, T. (1998) Cloning of cDNA Encoding a Novel Mouse DNA Topoisomerase III (Topo IIIbeta) Possessing Negatively Supercoiled DNA Relaxing Activity, Whose Message Is Highly Expressed in the Testis. *J. Biol. Chem.* **273**, 28553-28556

SHAIU, W. L., AND HSIEH, T. S. (1998) Targeting to transcriptionally active loci by the hydrophilic N-terminal domain of Drosophila DNA topoisomerase I. *Mol Cell Biol* **18**, 4358-4367

SHARMA, S., SOMMERS, J. A., WU, L., BOHR, V. A., HICKSON, I. D., AND BROSH, R. M., JR. (2004) Stimulation of flap endonuclease-1 by the Bloom's syndrome protein. *J Biol Chem* **279**, 9847-9856

SINGH, T. R., ALI, A. M., BUSYGINA, V., RAYNARD, S., FAN, Q., DU, C., ANDREASSEN, P. R., SUNG, P., AND MEETEI, A. R. (2008) BLAP18/RMI2, a novel OB-fold containing protein, is an essential component of the Bloom helicase-double Holliday junction dissolvasome. *Genes & Development*, 2856-2868

SRIVASTAVA, V., MODI, P., TRIPATHI, V., MUDGAL, R., DE, S., AND SENGUPTA, S. (2009) BLM helicase stimulates the ATPase and chromatin-remodeling activities of RAD54. *J Cell Sci* **122**, 3093-3103

SUGAWARA, N., GOLDFARB, T., STUDAMIRE, B., ALANI, E., AND HABER, J. E. (2004) Heteroduplex rejection during single-strand annealing requires Sgs1 helicase and mismatch repair proteins Msh2 and Msh6 but not Pms1. *Proc Natl Acad Sci U S A* **101**, 9315-9320

SUHASINI, A. N., AND BROSH, R. M., JR. (2012) Fanconi anemia and Bloom's syndrome crosstalk through FANCJ-BLM helicase interaction. *Trends Genet* **28**, 7-13

SUN, H., KAROW, J. K., HICKSON, I. D., AND MAIZELS, N. (1998) The Bloom's syndrome helicase unwinds G4 DNA. *J Biol Chem* **273**, 27587-27592

SUSKI, C., AND MARIANS, K. J. (2008) Resolution of converging replication forks by RecQ and topoisomerase III. *Mol Cell* **30**, 779-789

SZOSTAK, J. W., ORR-WEAVER, T. L., ROTHSTEIN, R. J., AND STAHL, F. W. (1983) The double-strand-break repair model for recombination. *Cell* **33**, 25-35

THORPE, H. M., AND SMITH, M. C. (1998) In vitro site-specific integration of bacteriophage DNA catalyzed by a recombinase of the resolvase/invertase family. *Proc Natl Acad Sci U S A* **95**, 5505-5510

TSE-DINH, Y. C., AND BERAN-STEED, R. K. (1988) Escherichia coli DNA topoisomerase I is a zinc metalloprotein with three repetitive zinc-binding domains. *J Biol Chem* **263**, 15857-15859

WALLIS, J. W., CHREBET, G., BRODSKY, G., ROLFE, M., AND ROTHSTEIN, R. (1989) A hyper-recombination mutation in S. cerevisiae identifies a novel eukaryotic topoisomerase. *Cell* **58**, 409-419

WANG, X., ZHANG, X., MAO, C., AND SEEMAN, N. C. (2010) Double-stranded DNA homology produces a physical signature. *Proc Natl Acad Sci U S A* **107**, 12547-12552

WANG, Y., CORTEZ, D., YAZDI, P., NEFF, N., ELLEDGE, S. J., AND QIN, J. (2000) BASC, a super complex of BRCA1-associated proteins involved in the recognition and repair of aberrant DNA structures. *Genes Dev* **14**, 927-939

WANG, Y., LYU, Y. L., AND WANG, J. C. (2002) Dual localization of human DNA topoisomerase IIIalpha to mitochondria and nucleus. *PNAS* **99**, 12114-12119

WEBB, M. R., PLANK, J. L., LONG, D. T., HSIEH, T. S., AND KREUZER, K. N. (2007) The phage T4 protein UvsW drives Holliday junction branch migration. *J Biol Chem* **282**, 34401-34411

WECHSLER, T., NEWMAN, S., AND WEST, S. C. (2011) Aberrant chromosome morphology in human cells defective for Holliday junction resolution. *Nature* **471**, 642-646

WEINERT, B. T., AND RIO, D. C. (2007) DNA strand displacement, strand annealing and strand swapping by the Drosophila Bloom's syndrome helicase. *Nucleic Acids Res* **35**, 1367-1376

WEINSTEIN, J., AND ROTHSTEIN, R. (2008) The genetic consequences of ablating helicase activity and the Top3 interaction domain of Sgs1. *DNA Repair (Amst)* **7**, 558-571

WILSON, T. M., CHEN, A. D., AND HSIEH, T. (2000) Cloning and characterization of Drosophila topoisomerase IIIbeta. Relaxation of hypernegatively supercoiled DNA. *J Biol Chem* **275**, 1533-1540

WU, J., FENG, L., AND HSIEH, T. S. (2010) Drosophila topo IIIalpha is required for the maintenance of mitochondrial genome and male germ-line stem cells. *Proc Natl Acad Sci U S A* **107**, 6228-6233

WU, L., BACHRATI, C. Z., OU, J., XU, C., YIN, J., CHANG, M., WANG, W., LI, L., BROWN, G. W., AND HICKSON, I. D. (2006) BLAP75/RMI1 promotes the BLM-dependent dissolution of homologous recombination intermediates. *Proc Natl Acad Sci U S A* **103**, 4068-4073

WU, L., CHAN, K. L., RALF, C., BERNSTEIN, D. A., GARCIA, P. L., BOHR, V. A., VINDIGNI, A., JANSCAK, P., KECK, J. L., AND HICKSON, I. D. (2005) The HRDC domain of BLM is required for the dissolution of double Holliday junctions. *The EMBO Journal* **24**, 2679-2687

WU, L., DAVIES, S. L., LEVITT, N. C., AND HICKSON, I. D. (2001) Potential role for the BLM helicase in recombinational repair via a conserved interaction with RAD51. *J Biol Chem* **276**, 19375-19381

WU, L., DAVIES, S. L., NORTH, P. S., GOULAOUIC, H., RIOU, J. F., TURLEY, H., GATTER, K. C., AND HICKSON, I. D. (2000) The Bloom's syndrome gene product interacts with topoisomerase III. *J Biol Chem* **275**, 9636-9644

WU, L., AND HICKSON, I. D. (2002) The Bloom's syndrome helicase stimulates the activity of human topoisomerase III{alpha}. *Nucl. Acids Res.* **30**, 4823-4829

WU, L., AND HICKSON, I. D. (2003) The Bloom's syndrome helicase suppresses crossing over during homologous recombination. *Nature* **426**, 870-874

XU, D., GUO, R., SOBECK, A., BACHRATI, C. Z., YANG, J., ENOMOTO, T., BROWN, G. W., HOATLIN, M. E., HICKSON, I. D., AND WANG, W. (2008) RMI, a new OB-fold complex essential for Bloom syndrome protein to maintain genome stability. *Genes & Development* **22**, 2843-2855

YANG, J., BACHRATI, C. Z., OU, J., HICKSON, I. D., AND BROWN, G. W. (2010) Human topoisomerase IIIalpha is a single-stranded DNA decatenase that is stimulated by BLM and RMI1. *J Biol Chem* **285**, 21426-21436

YANG, Q., ZHANG, R., WANG, X. W., SPILLARE, E. A., LINKE, S. P., SUBRAMANIAN, D., GRIFFITH, J. D., LI, J. L., HICKSON, I. D., SHEN, J. C., LOEB, L. A., MAZUR, S. J., APPELLA, E., BROSH, R. M., JR., KARMAKAR, P., BOHR, V. A., AND HARRIS, C. C.

(2002) The processing of Holliday junctions by BLM and WRN helicases is regulated by p53. *J Biol Chem* **277**, 31980-31987

YIN, J., SOBECK, A., XU, C., MEETEI, A. R., HOATLIN, M., LI, L., AND WANG, W. (2005) BLAP75, an essential component of Bloom's syndrome protein complexes that maintain genome integrity. *Embo J* **24**, 1465-1476

ZAKHARYEVICH, K., TANG, S., MA, Y., AND HUNTER, N. (2012) Delineation of joint molecule resolution pathways in meiosis identifies a crossover-specific resolvase. *Cell* **149**, 334-347

ZHANG, R., SENGUPTA, S., YANG, Q., LINKE, S. P., YANAIHARA, N., BRADSHER, J., BLAIS, V., MCGOWAN, C. H., AND HARRIS, C. C. (2005) BLM helicase facilitates Mus81 endonuclease activity in human cells. *Cancer Res* **65**, 2526-2531

Biography

Stefanie Lynn Hartman Chen (née Hartman) was born on December 7, 1983 in Frederick, Maryland. She attended Virginia Polytechnic Institute and State University (Virginia Tech) and graduated *summa cum laude* in May 2005 with a Bachelor of Science in Biochemistry and a minor in Animal and Poultry Sciences. She then joined the Department of Biochemistry at Duke University as a graduate student in August 2005. While there, she published a chapter entitled "Essential functions of Topoisomerase IIIα in the Nucleus and Mitochondria" in the book "DNA Topoisomerases and Cancer" (published by Springer, edited by Y. Pommier) and the peer-reviewed article "Essential functions of the C terminus of Topoisomerase IIIα in double Holliday junction dissolution" in the Journal of Biological Chemistry, both in 2012. The latter was selected by the journal as a Paper of the Week. Stefanie was also a fellow in the "Preparing Future Faculty" program during the 2010-2011 academic year. Her work has earned her a Kamin Poster Award at the annual departmental retreat and a travel scholarship to the TOPO 2011 international meeting in Taipei, Taiwan, both in the fall of 2011.